INFORMATION TO USERS

This reproduction was made from a copy of a document sent to us for microfilming. While the most advanced technology has been used to photograph and reproduce this document, the quality of the reproduction is heavily dependent upon the quality of the material submitted.

The following explanation of techniques is provided to help clarify markings or notations which may appear on this reproduction.

1. The sign or "target" for pages apparently lacking from the document photographed is "Missing Page(s)". If it was possible to obtain the missing page(s) or section, they are spliced into the film along with adjacent pages. This may have necessitated cutting through an image and duplicating adjacent pages to assure complete continuity.

2. When an image on the film is obliterated with a round black mark, it is an indication of either blurred copy because of movement during exposure, duplicate copy, or copyrighted materials that should not have been filmed. For blurred pages, a good image of the page can be found in the adjacent frame. If copyrighted materials were deleted, a target note will appear listing the pages in the adjacent frame.

3. When a map, drawing or chart, etc., is part of the material being photographed, a definite method of "sectioning" the material has been followed. It is customary to begin filming at the upper left hand corner of a large sheet and to continue from left to right in equal sections with small overlaps. If necessary, sectioning is continued again—beginning below the first row and continuing on until complete.

4. For illustrations that cannot be satisfactorily reproduced by xerographic means, photographic prints can be purchased at additional cost and inserted into your xerographic copy. These prints are available upon request from the Dissertations Customer Services Department.

5. Some pages in any document may have indistinct print. In all cases the best available copy has been filmed.

University Microfilms International
300 N. Zeeb Road
Ann Arbor, MI 48106

Order Number 1332415

Structural analysis of stretched membrane reflector modules using advanced composites

Ganapathy, Visvanathan, M.S.

The University of Arizona, 1987

U·M·I
300 N. Zeeb Rd.
Ann Arbor, MI 48106

PLEASE NOTE:

In all cases this material has been filmed in the best possible way from the available copy. Problems encountered with this document have been identified here with a check mark __✓__.

1. Glossy photographs or pages __✓__
2. Colored illustrations, paper or print _____
3. Photographs with dark background __✓__
4. Illustrations are poor copy _____
5. Pages with black marks, not original copy __✓__
6. Print shows through as there is text on both sides of page _____
7. Indistinct, broken or small print on several pages __✓__
8. Print exceeds margin requirements _____
9. Tightly bound copy with print lost in spine _____
10. Computer printout pages with indistinct print _____
11. Page(s) _____ lacking when material received, and not available from school or author.
12. Page(s) _____ seem to be missing in numbering only as text follows.
13. Two pages numbered _____. Text follows.
14. Curling and wrinkled pages _____
15. Dissertation contains pages with print at a slant, filmed as received _____
16. Other _____

_____

_____

STRUCTURAL ANALYSIS OF STRETCHED MEMBRANE REFLECTOR MODULES USING ADVANCED COMPOSITES

by

Ganapathy Visvanathan

A Thesis Submitted to the Faculty of the

DEPARTMENT OF AEROSPACE AND MECHANICAL ENGINEERING

In Partial fulfillment of the requirements
For the Degree of
MASTER OF SCIENCE
In the Graduate College

THE UNIVERSITY OF ARIZONA

1 9 8 7

STATEMENT OF AUTHOR

This thesis has been submitted in partial fulfillment of requirements for an advanced degree at the University of Arizona and is deposited in the University Library to be made available to borrowers under rules of the Library.

Brief quotations from this thesis are allowable without special permission, provided that accurate acknowledgement of source is made. Requests for permission for extended quotation from or reproduction of this manuscript in whole or in part may be granted by the head of the major department or the Dean of the Graduate college when in his or her judgement the proposed use of the material is in the interests of scholarship. In all other instances, however, permission must be obtained from the author.

SIGNED: BDarakan

APPROVAL BY THESIS DIRECTOR

This thesis has been approved on the date shown below:

R. N. Kumar

Dr. Kumar Ramohalli
Associate Professor of Aerospace
and Mechanical Engineering

12/15/87

Date

ACKNOWLEDGMENTS

I wish to express my sincere appreciation to Dr. Kumar Ramohalli for his valuable advice and guidance that I received throughout the research and writing of this thesis.

I acknowledge and express my gratitude to Dr. Kamel and Dr. Joshi, faculty members of the Aerospace and Mechanical Engineering Department at the University of Arizona, who shared not only their expertise but encouragement, understanding, and support through this study and research.

Acknowledgements are also due to Mr. Benamanahalli Nagraj, Mr. Ramchandar Nagulpally and Mr. Tony Mobley of Casa Gifts for great help in computer modelling using GIFTS. I am extremely grateful to Mr. Nelson Zabik and his colleagues, Mr. Dave Wright, Mr. Gary Hopkins, and Mr. Lorenzo Lujan of the Aerospace and Mechanical Engineering Machine Shop, for their help in experimental work. They were always willing to help and I sincerely acknowledge their help above and beyond the call of duty.

I would like to extend my sincere thanks to my friends Rambabu, Jaywanth, JoAnn, and Rajesh for proof reading and typing this manuscript. They provided valuable suggestions and assistance in the preparation of this thesis. I thank Afzal for helping me with the sketches.

I owe my special thanks to all my predecessors upon whose work I have drawn extensively.

Also, I wish to express my appreciation and gratitude to Mr. John Roach of 3M-Minnesota, for providing the material for the experimental work free of cost and whenever it was required.

The research in this study was funded by the Solar Energy Research Institute, Golden, Colarado, as subcontract No. XK-6-06037-1.

TABLE OF CONTENTS

CONTENTS...Continued

LIST OF ILLUSTRATIONS

ILLUSTRATIONS...Continued

LIST OF TABLES

ABSTRACT

The concept of achieving low cost ($\approx \$20/m^2$) and ultra low weight ($5\ kg/m^2$) for heliostats is explored theoretically and experimentally. The objective of this work is to significantly improve the cost and performance of the structure under concern, without sacrificing strength and efficiency.

The focus is on an innovative design of stretched-membrane heliostats. A reflective membrane of thin film is supported by a taut fishnet structural membrane consisting of graphite fiber-polymer matrix composite. The reflective and structural membranes are attached to a ring frame made of wood.

The nonlinear problem of stress-strain analysis is formulated and solved using the finite-element code NASTRAN. The analysis is done for loads which include the initial stretching of the film and structural membrane and the pressure load due to wind. The scope of the present work is limited to analyzing the structural deformation behavior of flat-plate heliostats and partial extension to parabolic and semi-hemispherical dish reflectors.

CHAPTER 1

INTRODUCTION

The importance of low-cost solar thermal energy has been discussed in the literature in the specific context of reflector technology [1]. Various technical approaches to fabricating reflectors were compared in a concise way [2]. It is recognized that before widespread use can be seen, considerable reductions in the cost of reflectors are necessary. A technology for achieving this without sacrificing the strength, stiffness, and service life of the reflectors was the goal of the present research.

Glass, metal, and related technologies have been compared and shown to be capable of weighing 5 kg/m^2 (1 lb/ft^2) of collector area. In addition, the current and future projections seem to indicate a cost greater than $\$100/m^2$ ($\$9.30/ft^2$) for this popular technology. Several modifications can be explored, to produce lower costs for this basic, well proven technology. A revolutionary new design is needed to achieve cost figures of $\$20\text{-}30/m^2$($\$2\text{-}3/ft^2$). The basic philosophy of this work is centered around efficient use of modern high-tech materials and the design tools available for their fabrication. The technology is closely related to the stressed-membrane concept pioneered at the Solar Energy Research Institute (SERI) [1]. In addition, the new structural design innovation [3] of stressed fiber fishnet played a crucial role in greatly reducing the costs and weight. An over-simplified analogy for the new technology would be a tennis racquet, with its taut strings providing stiffness, covered by a stressed membrane. This design allows extremely efficient material utilization, since the tensioned fibers operate close to their ultimate yield strengths and the membrane material is stressed only moderately. The ring frame to which the stressed membrane and the fibers are attached is subject to nearly

radial compression, allowing for an extremely efficient use of materials. Another advantage is that larger diameter (15m) reflectors are feasible, in contrast to the designs without fibers.

It is easily appreciated that this new technology has not been analyzed before. The analysis of this highly nonlinear problem requires a good computer code, and good physical insight into modelling. While the product is certainly a composite, it is not possible to readily apply the usual composite-material analysis codes because of the very low (5%) fiber "filler" within the continuous "matrix" of the membrane. In addition, the membrane does not occupy the same plane as the fibers and this introduces a new dimension to the problem. The goal of this analysis is to identify the fundamental physical processes and to develop working codes to predict the performance of both in-plane and out-of-plane membrane-fiber net deflection due to the initial tensioning and possible normal loads due to wind. It was also the objective of this work to use analytical techniques for the optimal design and the construction of these modules. For example, the analysis must answer questions concerned with

1. the number of directions of the fiber runs,
2. the spacing of the fiber runs,
3. the thickness of the fibers,
4. material of the fibers,
5. thickness of the membrane(s) and related parameters.

The design code must also enable a selection of the ring-frame cross section. Thus, the overall purpose of this research was to understand the structural behavior of the reflector modules fabricated with advanced composites, and to provide some information for defining the limits of acceptable deformations, geometry, and design parameters, which are required to control the membrane surface to the desired accuracy from an optical perspective.

Double-membrane design with a thin reflective film and graphite fiber-polyimide resin with a spacing of 10 mm between adjacent runs of fibers attached a wooden frame, was analyzed in this research. ECP-91 polymer film was used as the reflective membrane. The results obtained in this particular research work are for 0.2-m, 1.2-m, and 2-m diameter flat heliostat modules. The results are summarized in Table 4.1.

The model behavior is described in Chapter 2. The design analysis is presented in Chapter 3, the results are discussed in Chapter 4, and a preliminary cost analysis is given in Chapter 5. The summary and conclusions are provided in Chapter 6.

Parabolic dish reflectors were built to prove the concept of composite-membrane technology. The fabrication process for the parabolic reflectors is described in Appendix C. Some analytical solution procedures for single- and double-membrane reflectors are given in the references [4-6].

The finite-element model analyzed in this study provided some understanding of the structural response of the double-membrane combined with the composite support structure. The deflections obtained here give an insight to the membrane response to design loads such as in-plane tension and normal wind loads. The experimental construction of the parabolic dish reflectors indicated problems which may arise during fabrication of composite membranes. A code of procedure was established for finite-element analysis of special structures such as the one considered here. Although this analysis revolved around the use of one of the popular nonlinear structural analysis codes (NASTRAN), it can use other nonlinear techniques as well.

CHAPTER 2

PROBLEM DESCRIPTION

Stressed-Membrane Concept

The stressed-membrane concept initiated at SERI was the major element of this innovative design. At first, a single stressed-membrane of reflective film, polymeric in nature, stressed over a hollow torroidal frame was considered. Fig. 1 shows the idealized stressed membrane reflective module with axisymmetric supports. Analytical studies were conducted and accuracy of the results was compared with the results from the NASTRAN code. An optical-surface error model was also developed and applied to translate frame and membrane deformations into quantifiable tolerances for the assembly. The results of the study led to the development of a double-membrane approach, as shown in Fig. 2. The double-membrane concept improved on the single-membrane design as shown below:

- Unlike the single-membrane designs, the double-membrane approach couples the in-plane membrane material stiffness with the deformation process even at low loads and low tension levels.
- Because of this stiffness-deformation coupling, the double-membrane module is considerably stiffer to lateral loads due to wind pressure than the corresponding single-membrane design.
- Membrane attachment has a significant impact on the reflector module. If the membrane is attached to the frame so that its plane does not pass through the frame shear center, an initial twist of the frame will be present prior to lateral pressure loading. This initial twist can amplify the out-of-plane deformations

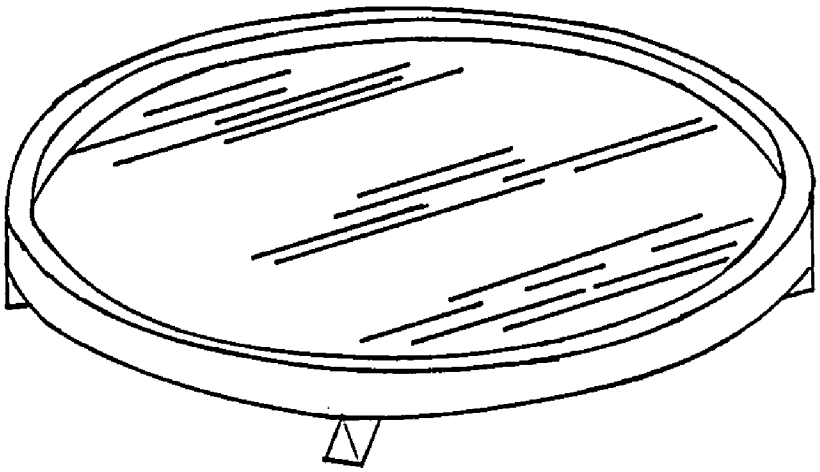

Figure 1. Perspective View of Stretched-Membrane Reflective Module Supported at Four Equidistant Circumferential Points. (Top Membrane and Fishnet Backing Removed for Clarity)

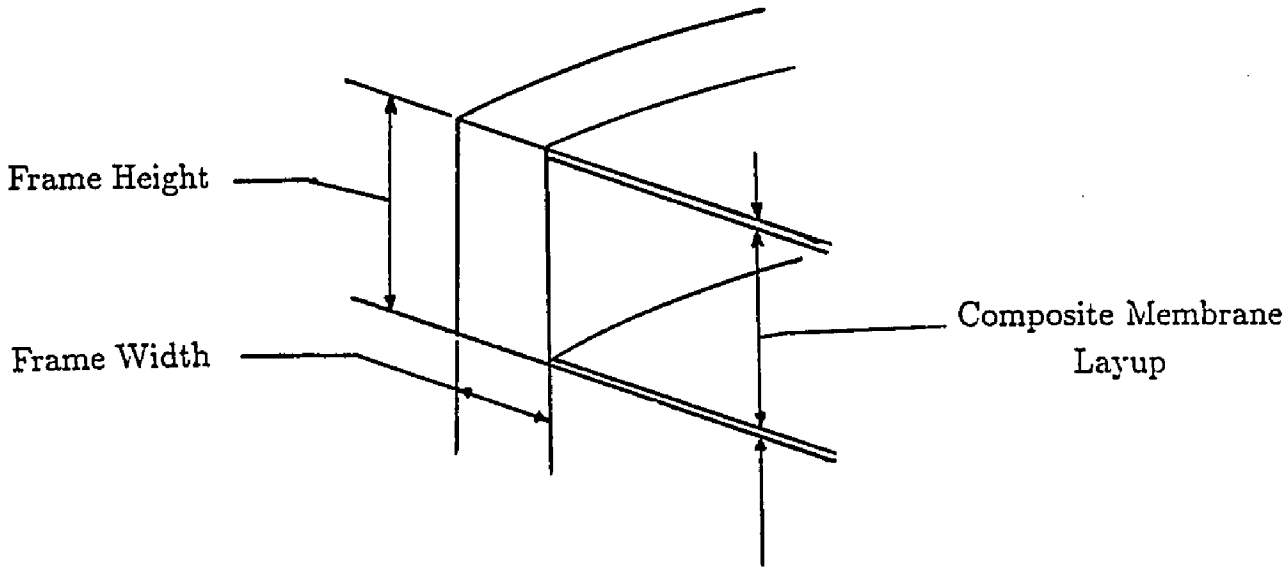

Figure 2. Cross-Sectional View of Double-Membrane Design for Wood Frame-Membrane Combination.

and can induce peak bending stress in the frame. With the double-membrane design, the membranes were placed symmetrically with respect to the centroid plane of the frame. This provides an additional flange to the frame which in turn reduces the frame rotations.

- The axisymmetric sag of the membrane due to wind-induced pressure loading led to significantly more optical error than the effect due to nonsymmetric membrane deformations. These nonsymmetric deformations were caused by periodic support constraints. This axisymmetric effect can almost be eliminated using double membranes.

Based on the above findings, it was decided to develop the double-membrane concept with advanced composites as backing for the reflective film to provide a light weight, low cost, and structurally efficient design.

The cross sectional view of the double membrane design shown in Fig. 2 consists of two membranes placed symmetrically on either side of the rectangular frame. The initial tension of each membrane was assumed to be exactly one half of the total tension. The torroidal frame is supported at four equidistant points around the periphery of the frame. In the present study, graphite fibers in polyimide resin were initially stressed and attached to the frame. The polymeric reflective film membrane was stressed over the taut graphite fibers and attached to the frame. The pre-tensioned graphite fibers serve as structural backing for the reflective film, providing additional stiffness to the membrane.

Geometric Nonlinearity

If the load-deformation process is assumed to be linear, using elementary linear analysis, the load deformation response for a circular membrane fixed at radius a, under constant tension, is given by

$$w = w_o \left[1.0 - (\frac{r}{a})\right], \tag{1}$$

where the center displacement w_o is given in terms of the nominal focal length and load by

$$w_o = \frac{a^2}{4f} = \frac{Pa^2}{4T_o}. \tag{2}$$

The uniform pressure, P, was assumed to act normal to the plane of the membrane in the direction w, and f is the nominal focal length for the curved reflector. For parabolic surfaces, f is constant. From a structural perspective, this simple linear solution for w results from a geometric stiffness effect alone, as there are no material properties in this load-deformation relationship. Thus, in this case the membrane carries the lateral load by changing shape. Eqs. (1) and (2) give an upper bound on the displacement field, since the membrane does strain with lateral deformation, thus increasing the tension in the membrane. This additional strain is done within the structure and helps retard the motion of the membrane. If the membrane behaved as shown in Eqs. (1) and (2), then the problem is easily solved using the simple linear relationship. However, the membrane behaves differently, and the linear solution does not answer the majority of focussing design considerations that are specially associated with typical applications such as the reflectors considered here.

Therefore, to accurately predict the optical/structural response of the membrane surface, the more general nonlinear load-deformation problem must be considered. The membrane tension does not remain constant, but varies over its surface as it distorts out of its original plane due to the lateral wind pressure, which was assumed to be uniform. For instance, at its fixed edge, $r = a$, the net strain in

the radial direction increases, but circumferentially the net tension is constrained to remain fairly constant. In the center region of the membrane, both the resulting strain and stress components increase uniformly as there is additional strain in the membrane during deflection. When the appropriate nonlinear problem is considered, the associated changes in tension can be determined and their effects defined along with the resulting change in the surface shape. This change in tension of the membrane results in change in the slope, and deforms the membrane out-of-plane. This deformation is larger than the membrane thickness. Hence the problem is treated as geometrically nonlinear, but the material properties are assumed to be linear.

Solution Method

The use of pretensioned laminated membranes has been recognized as a very effective way of using the material where transverse deflection and slope are critical design considerations. Loading the pretensioned membrane laterally results in moderate to large deformations. The large deformations considered here result from satisfying focussing requirements.

Small elastic deformations of membranes and thin shells and also moderate to large elastic deformations are well documented in literature [9]. Moderate to large elastic deformations have also been presented separately[5, 10]. These are restricted to isotropic membranes only, and are based on variation procedures yielding load-deformation relationships. The Rayleigh-Ritz technique could be applied, assuming a parabolic transverse displacement. The analytical formulation cannot provide deviation from the assumed parabolic shape, and therefore one has to resort to numerical studies to study the variation. Above all, the problem considered here, a stressed-membrane heliostat attached to a torroidal frame, supported at four

equidistant points along the periphery of the ring, and using a new material, is a special type, for which no ready-made solutions are available. Preliminary studies on single and double membranes have indicated that the interaction between the frame and the membrane, the attachment of membranes to the frame, and the support conditions play a vital role in obtaining the desired load-deformation characteristics, which have a direct impact on the focal length of the heliostats.

Nonetheless, various finite element methods used by Cook [11] and Fried [12] for large-membrane deformation analysis can be adapted for analytical solution of this problem. However, these finite element methods give a general solution for isotropic and rubber-like materials and have limitations on the support conditions, which are more general in nature, such as fixed, simply supported, or hinged conditions. It would also be difficult to analyze the laminated membrane with the torroidal frame and to match the load-deformation response of the frame and the membrane. Iterative procedures using finite difference methods could be used, but would be highly tedious and time consuming, especially when dealing with a nonlinear problem such as this.

Therefore, one has to resort to other numerical methods to solve the problem, the results of which provide insight into the importance of various parameters associated with the problem. Though there are several approaches to solving this nonlinear problem, the easiest and most straightforward approach is to use a finite element analysis code available on the market. One such finite element code, NASTRAN, is for general structural analysis and a versatile code, capable of analyzing composite materials and structures. However, finite element analysis is quite expensive and cumbersome. The most important aspect is the success of the procedure through proper convergence of the solutions. This required six months of careful work with the NASTRAN code.

CHAPTER 3

DESIGN ANALYSIS

Model Description

The model for the analysis, shown in Fig. 3, consists of a composite membrane, stretched over a circular ring of wood. Reinforcement was provided for the reflective polymer film by graphite fibers under initial tension. Three layers of fibers were assumed, with orientations of $0^o/60^o/\text{-}60^o$ and equal spacing between the adjacent runs of fibers. The composite membrane was attached on both sides of the frame. Four symmetric equally-spaced supports were provided at the outer periphery of the frame.

The initial tension of the membrane was assumed to be shared by both membranes equally. The wind load was assumed to be uniform and applied as lateral pressure on one side of the membrane only.

Model Assumptions

- One quarter of the module was investigated, to take advantage of symmetry in the pretensioned state.
- ECP-91 polymer film, manufactured by 3M, of thickness 76μm, was used as the reflective-film membrane.
- A wooden frame of rectangular cross section was used for the circular ring frame. For example, for a

  0.2-m diameter module, the cross-section used was 12.7 × 10.16 mm, a

  1.2-m diameter module, the cross-section used was 20.0 × 16.00 mm, and a

  2.0-m diameter module, the cross-section used was 63.5 × 35.56 mm.

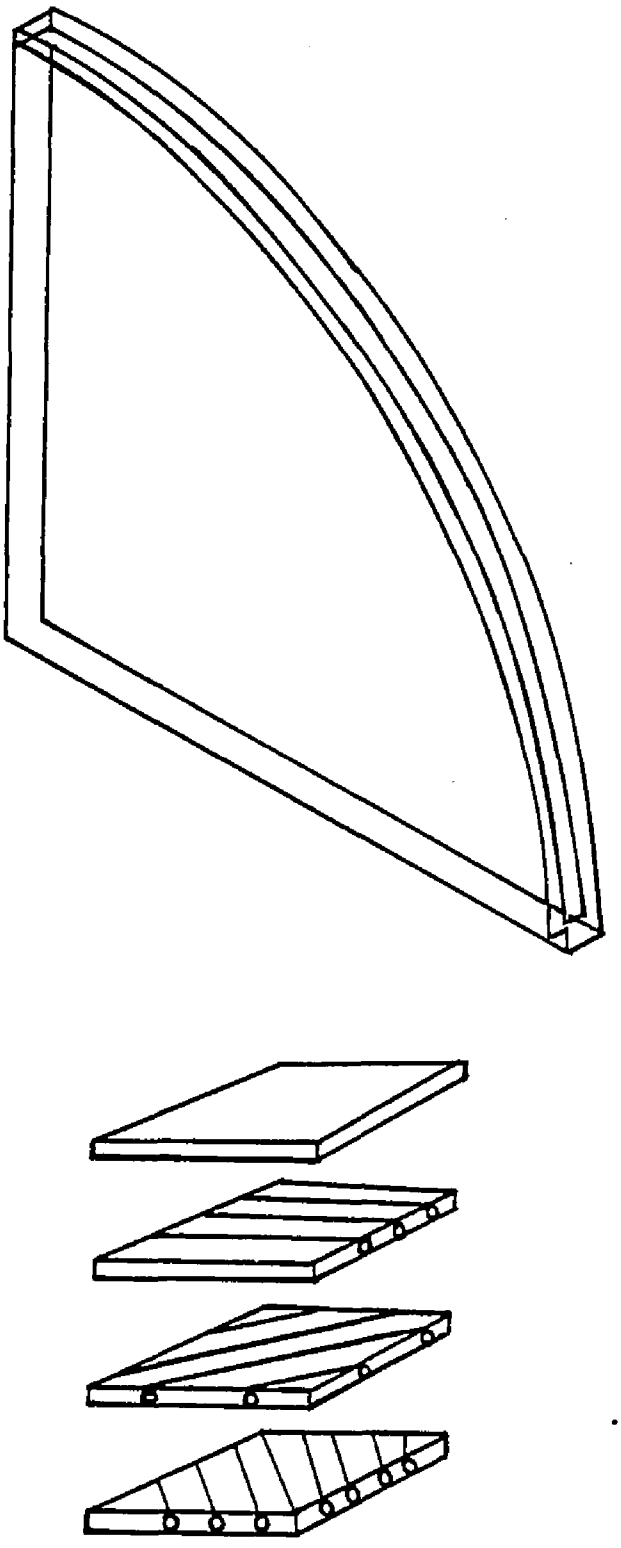

Figure 3. Hypothesized Model for NASTRAN

- Graphite fibers in polyimide resin, with a spacing of 10 mm between adjacent runs of fibers, were assumed.
- A combined stress of 50,000 psi was assumed as the initial stress on both the fibers and the reflective membrane.
- Load due to wind pressure was assumed to be uniform and three different values, 30, 60, and 90 Pa, were used.
- The out-of-plane displacement of the composite membrane is large and the strains are small. Also, the composite membrane thickness is small compared to the displacement in the transverse direction. Therefore, small strain-large displacement theory was assumed. This problem was treated as geometrically nonlinear. However, the material behavior was assumed to be linear.
- Only out-of-plane deformations of the ring and membrane were considered of importance here. This importance arises from the focussing requirements as the out-of-plane deformation would influence the focal length of the reflector.

Finite Element Model

To reduce the problem solution time and the computer disk space, a model as simple as possible is preferred. For the finite element analysis, the symmetry of the model and load was used. The actual model has symmetry in two planes. Therefore, the best possible reduction would be to a quarter-size model. Since we have four symmetrical supports, the support constraint could also be modelled using the quarter model.

Eight-noded solid elements were used for the frame cross section. Triangular and quadrilateral membrane elements were used for modelling the composite membrane. The fibers were assumed to be soaked in polyimide resin. Due to the fishnet layup of the fibers, an imaginary matrix is assumed between the adjacent fiber runs.

It should be understood that the fibers and the reflective film membrane do not lie in the same plane. For the composite layup of reflective film membrane and the fibers, four layers of material with appropriate thickness, material properties, and orientation were input as the data for the analysis. The initial tension in the membrane and fibers is recomputed as equivalent line load and are applied at both the radial arms of the quarter model. Wind load, assumed to be uniform, is applied as pressure load normal to the plane of the composite membrane. Symmetric boundary conditions are applied at the radial arms. The support is such that the frame is free to rotate but the translation in the perpendicular direction is restrained. Only two support points figure in the quarter model, and due to symmetry, all the translational degrees of freedom are restrained at the supports.

The model is generated using GIFTS finite element package. GIFTS has a pre-processor, which helps to visualize the model for correctness before analysis. Through an interface routine, the model generated using GIFTS is coded into NASTRAN input data for the analysis. The model generation is briefly explained and a sample NASTRAN input file is given in Appendix A. The analysis of the overall module, shown in Fig. 1, is for a specific case of three runs with the fibers at $0^o/60^o/-60^o$. In order to use the composite material analysis capability of NASTRAN, an imaginary matrix was assumed around the fibers, with the matrix strength and stiffness contributions set to zero.

The graphite fiber in a polyimide matrix was taken to be 50% by volume fraction. The polymer membrane film was ECP-91 with a thickness of 76μm. Thus, the elastic constants (Young's modulus, bulk modulus, and Poisson's ratio) were calculated by the rule of mixtures. The model for anlysis is shown in Fig. 3. Note that volume fraction, V_f, of the fiber is given by

$$V_f = A_f/A_c, \tag{3}$$

while the volume fraction of the (imaginary) matrix V_m between fiber is

$$V_m = A_m/A_c \equiv 0. \tag{4}$$

Here, A_f, A_m, and A_c, are the cross sectional area of the fiber, matrix, and the fiber-matrix composite, respectively. This enabled the unambiguous calculation of the input properties (see Appendix A). The 2-m diameter module with a wood frame of dimensions shown in Fig. 1 and supported symetrically on four equidistant (90°) supports was analyzed. The results included both in-plane and out-of-plane deformations, with typical initial tension values shown in Figs. 4, 5, and 6, and a normal wind load of 30-90 Pa.

Geometric Nonlinearity in NASTRAN

Geometric nonlinearity means that the relationship between strains and displacements is nonlinear. The NASTRAN solution algorithm for such a case is an extension of the differential stiffness approach. The differential stiffness approximation uses upto four terms in the strain-displacement relationship. The consideration of differential stiffness effects can provide an improved solution relative to linear elastic solutions which is adequate for many problems. The linear elastic and the differential stiffness solutions are the first two iterations in the geometrically nonlinear algorithms, which is an iterative techniques utilizing a modified Newton-Raphson method.

The geometrically nonlinear solution in NASTRAN is based upon an exact solution of the equations of equilibrium. These elements are formed to allow large element deflections as long as the distortions are small. The formulation requires an exact nonlinear relationship between displacements and strains.

The approach requires a displaced element coordinate system to be constructed for each element, which follows and rotates with the element as the model deforms.

Changes in the shape of the element (distortions) are treated as displacements with respect to the displaced element coordinate system. Rigid-body displacements and rotations do not contribute to the distortions. In the displaced element coordinate system, the distortions are small, and linear elastic theory can be used. Element forces in the displaced element coordinate system are computed by simply pre-multiplying the displacements by the elastic (small motion) stiffness matrix. The incremental stiffness matrix, when expressed in the displaced element coordinate system, is the sum of the elastic and differential stiffness matrices. Applied loads are computed using the displaced geometry, which allows the inclusion of "follower" forces in the model.

The key equation is

$$[K^m]\{u^{n+1} - u^n\} = \{P^l - F^n + Q^{n+1}\} \tag{5}$$

Eqn. (5) is the modified Newton-Raphson algorithm used to solve the equilibrium condition, where F = vector of element forces

K = matrix of incremental stiffness

P = vector of applied loads

Q = vector of forces of constraint

u = displacement vector

n = loop counter

l = last loop when loads are updated

m = last loop when matrices were updated

Eqn. (5) is used only for the third and successive iterations. The first two iterations correspond exactly to the solution procedure used in differential stiffness. When the convergence is achieved, F = P + Q. This means that the element forces are in equilibrium with the element loads for all free degrees of freedom in the model.

CHAPTER 4

RESULTS AND DISCUSSION

Results

The results presented in this section are for 0.2-m and 2-m diameter modules. The initial tension of 16775 N/m on the composite membrane was assumed to be equally split between both membranes. The circular ring frame is made of wood. The frame cross sections for modules of different diameters are shown in Fig. 4. The structure is supported at two points and the details are shown in Fig. 5. Pressure load was applied normal to the surface on one of the membranes. This load was superimposed on the in-plane tension computed as shown in Appendix B, which was applied as line load, shown in Fig 6. The model was analyzed using NASTRAN for nonlinear load-deformation response. The solution was iterated until convergence.

All the results presented here are for graphite-polyimide fiber-resin matrix with 10-mm spacing between adjacent runs of fibers. Three runs of fibers were used, oriented at $0^o/60^o/-60^o$. The membrane is the fourth layer on top of the fibers. The load was applied on one side of the membrane only, but on the other side the same configuration of the composite membrane layup is maintained for symmetry.

Flat circular membranes were considered. Since a quarter model was used, only two support points come into consideration. Vertical translation of the frame is restrained at the support points. Also, only the outside nodes are restrained at the support points. Due to symmetry, at the support points translations in the plane normal to the surface are restrained at the support points. Figs. 5 and 6 show the boundary and loading conditions.

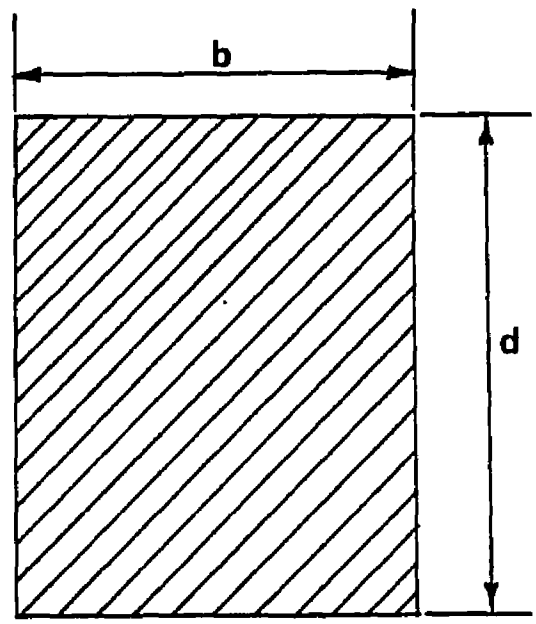

Module Dia.	d	b
(m)	(mm)	(mm)
0.20	12.70	10.16
1.20	20.00	16.00
2.00	63.50	35.56

Figure 4. Frame Cross Sections for Different Module Diameters

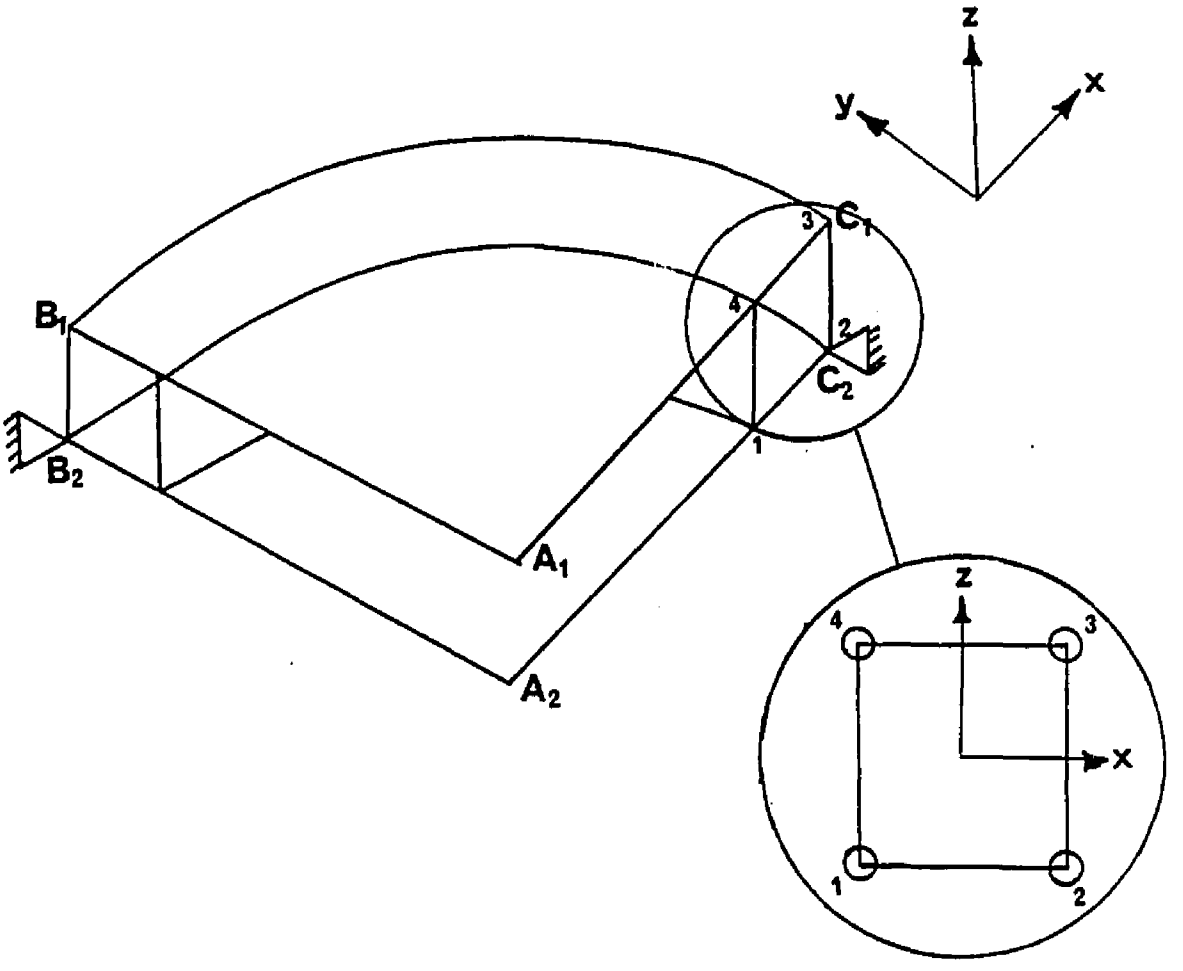

Boundary Conditions

Edges A_1B_1 and A_2B_2 – x translation restrained.
Edges A_1C_1 and A_2C_2 – y translation restrained.

Refer to Insert

Node 2 - x, y, z translations restrained.
Similarly, node at B_2 x, y, z translations restrained.

All rotational degrees of freedom are restrained.

Figure 5. Perspective View of the Quarter Model Showing the Applied Boundary Conditions.

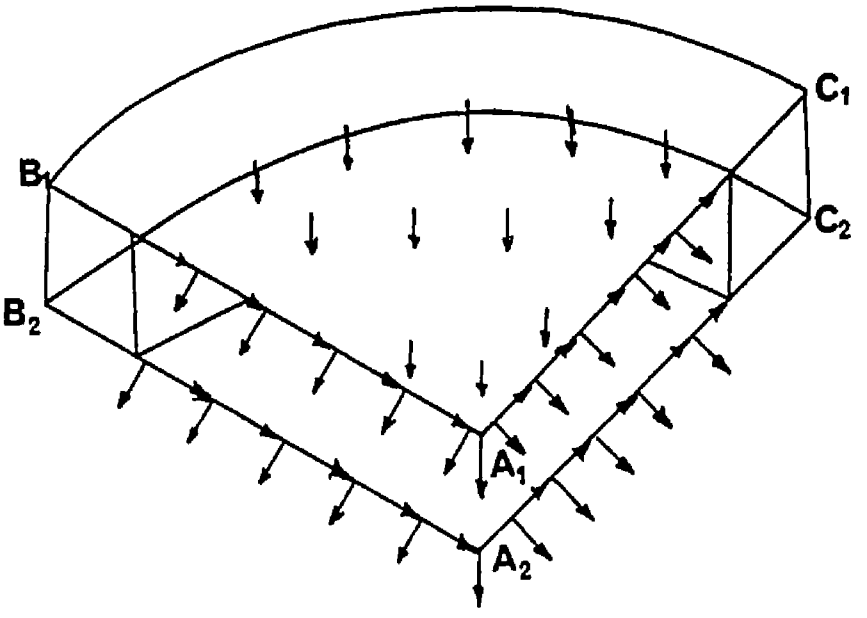

Applied Loads

On edges A_1B_1 and A_2B_2 and edges A_1C_1 and A_2C_2
line loads are applied as equivalent of initial tension.
On top surface $A_1B_1C_1$, uniform pressure load
equal to the normal windload is applied.

Figure 6. Perspective View of the Quarter Model Showing the Applied Loads.

The results include both in-plane and out-of-plane deflections with typical initial tension values as shown in Figs. 7–12, and a normal wind load of 30-90 Pa.

Figs. 7 and 8 show the in-plane deflections of the frame for the 0.2-m and 2-m diameter modules, respectively. The deflections are plotted as a function of angular distance between the supports. The deflections u and v correspond to the x-y global coordinate system and [u + v] corresponds to the vectorial sum of u and v.

It is seen from the graphs that the u and v deflections are not exact mirror images of one another. The values are positive in the v-direction intially and negative in the u-direction. At 45°, exactly halfway between the supports, the direction changes. The difference in the magnitudes of u and v is attributed to different tension values in the x- and y-directions. At 0° the component of tensile force in the y direction is greater than the tensile force in the x-direction. This magnitude varies as the angular displacement changes from 0° to 90°, and at 45° the direction also changes. Hence, we see the change in the values on the graph.

The in-plane frame deflections are not as significant as the out-of-plane deflections. From the results, it is seen that they are negligible when compared to the out-of-plane deflections, as shown in the subsequent Figs. 9–12.

The out-of-plane deflections seen in Figs. 9 and 10 are plotted for the frame as a function of the angular distance, as in the previous case. The figures show a perfect symmetry, which is expected since the maximum deflection is at the midpoint between the supports. The values shown are for different wind-pressure loads from 30-90 Pa. These out-of-plane deflections are significant, as they could amplify the out-of-plane deflections of the membrane. This affects the focal length of the reflector modules. Therefore, limiting the frame out-of-plane deflections is

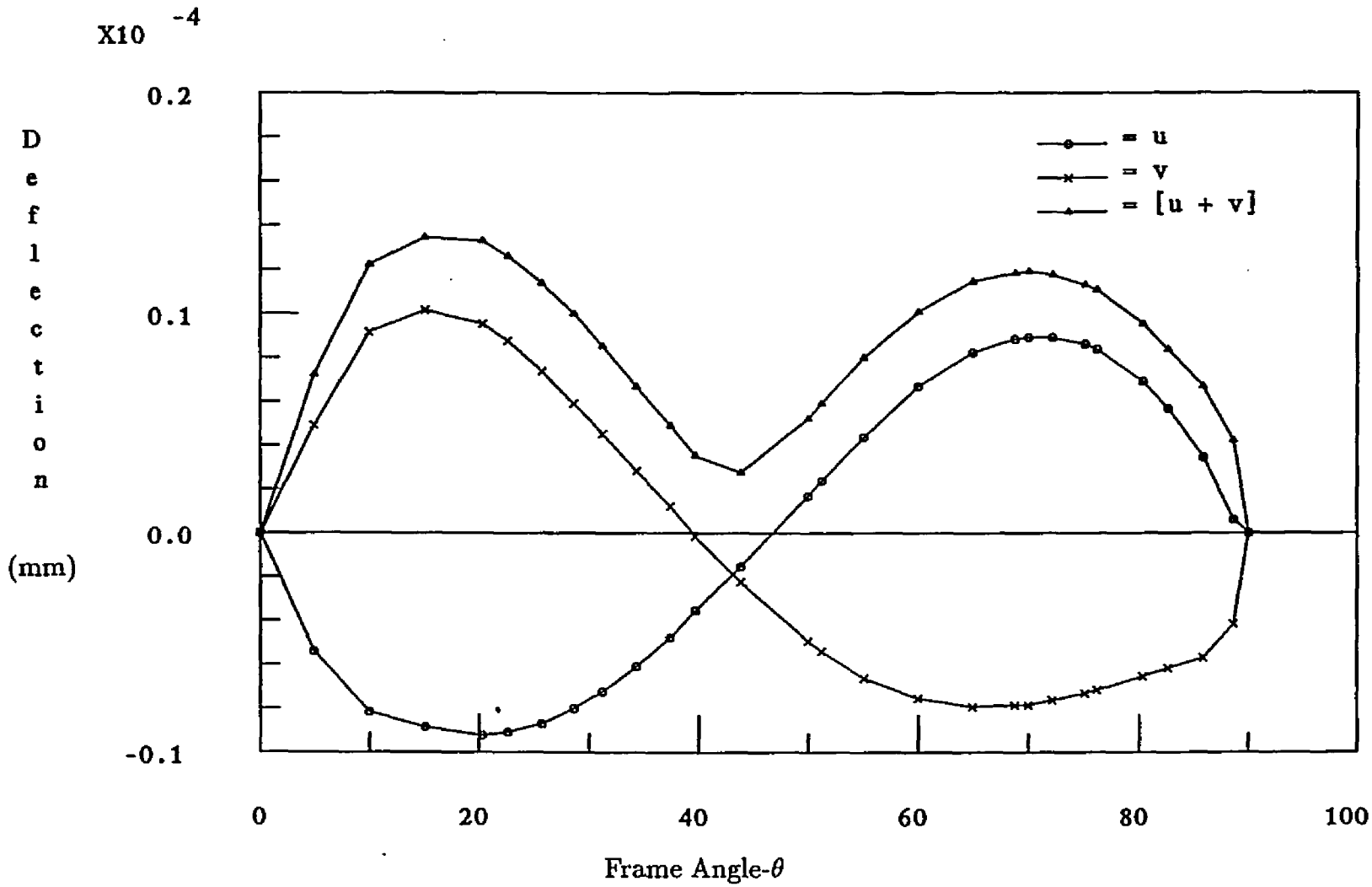

Figure 7. In-Plane Deformation of Frame as a Function of Angular Distance Between the Supports for 0.2-m Dia. Module. (Initial Tension = 1677.5 N/m, Wind Pressure = 30-90 Pa).

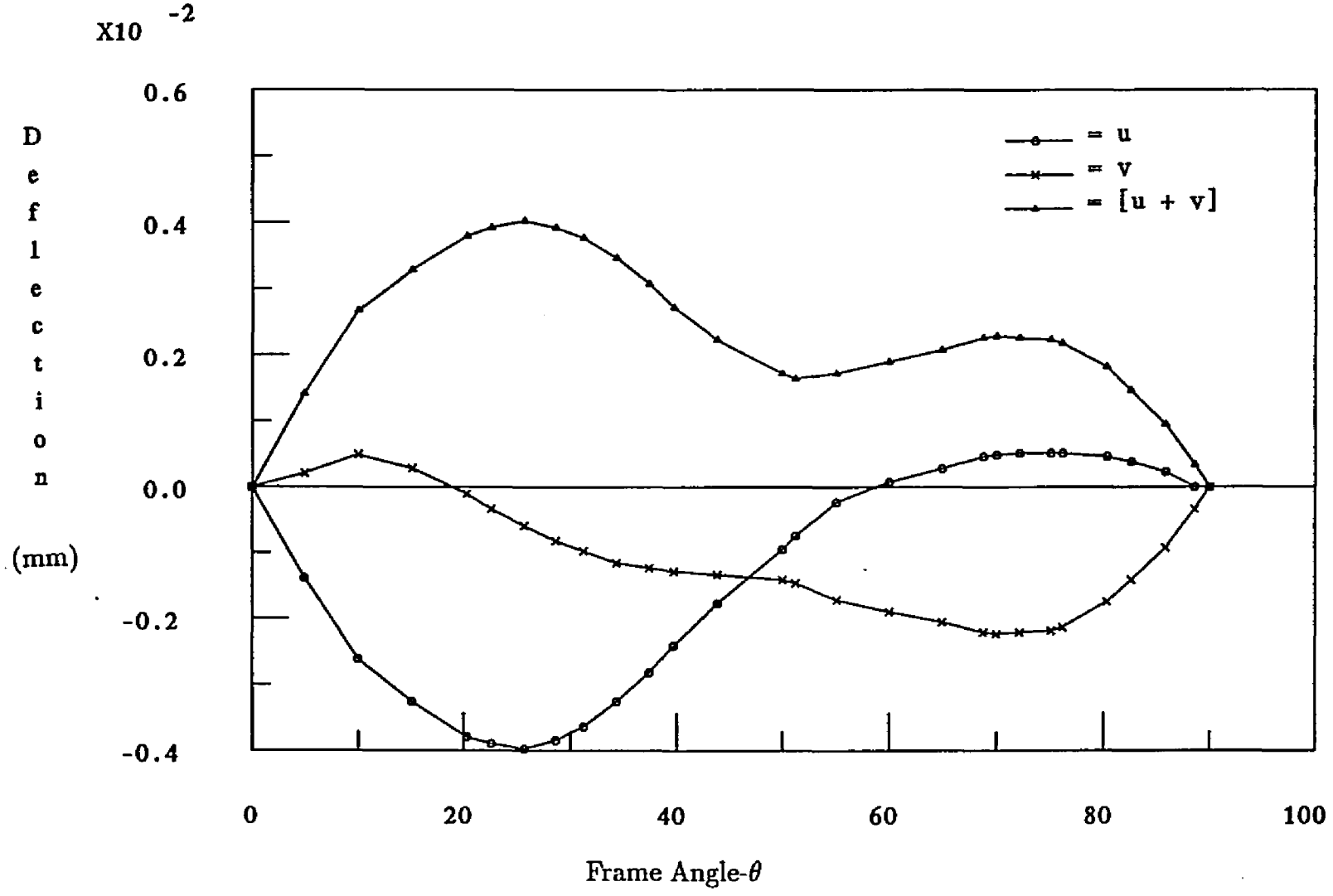

Figure 8. In-Plane Deformation of Frame as a Function of Angular Distance Between the Supports for 2.0-m Dia. Module. (Initial Tension = 16775 N/m, Wind Pressure = 30-90 Pa).

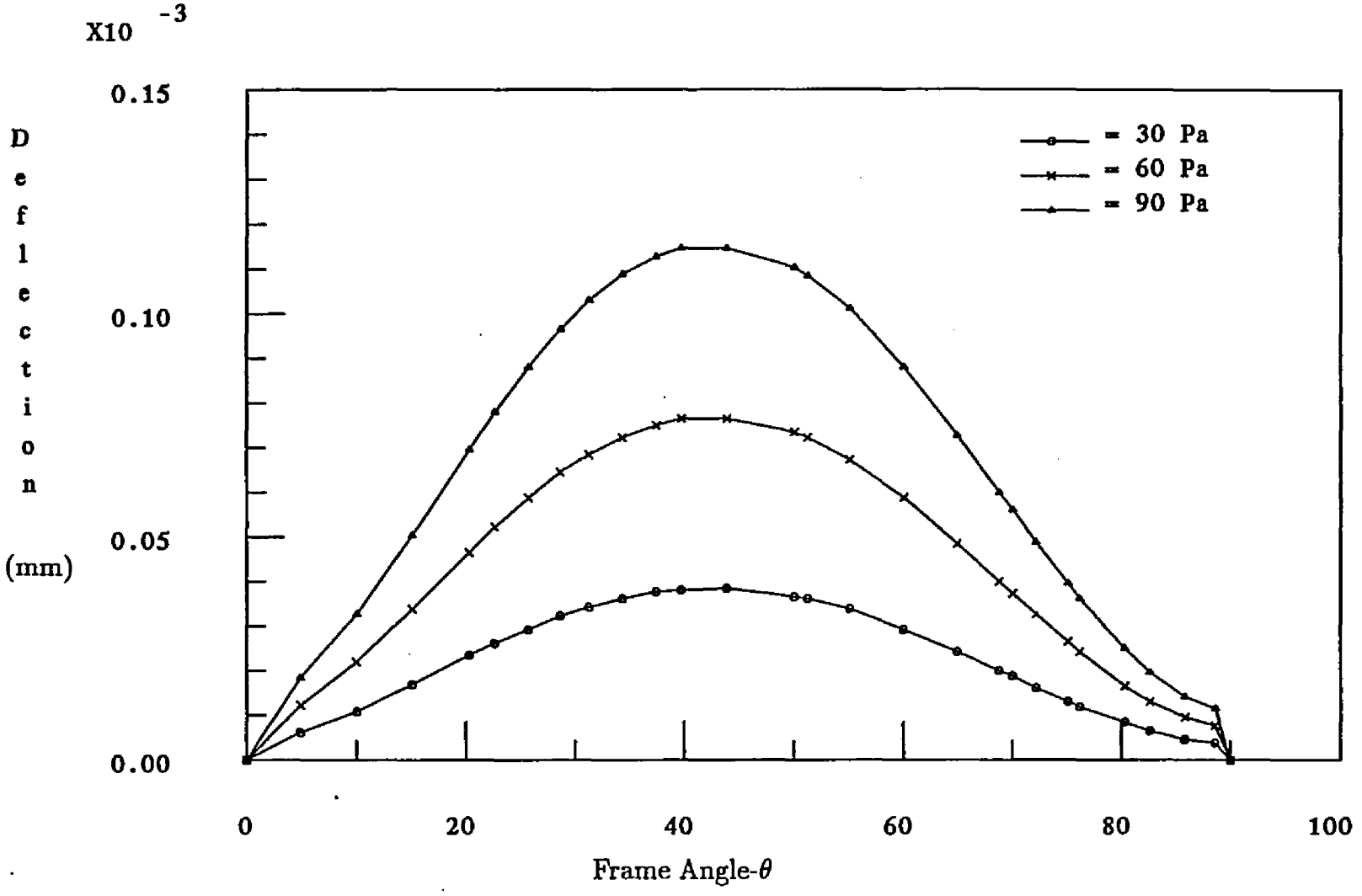

Figure 9. Out-of-Plane Deformation of Frame as a Function of Angular Distance Between the Supports for 0.2-m Dia. Module. (Initial Tension = 1677.5 N/m, Wind Pressure = 30-90 Pa).

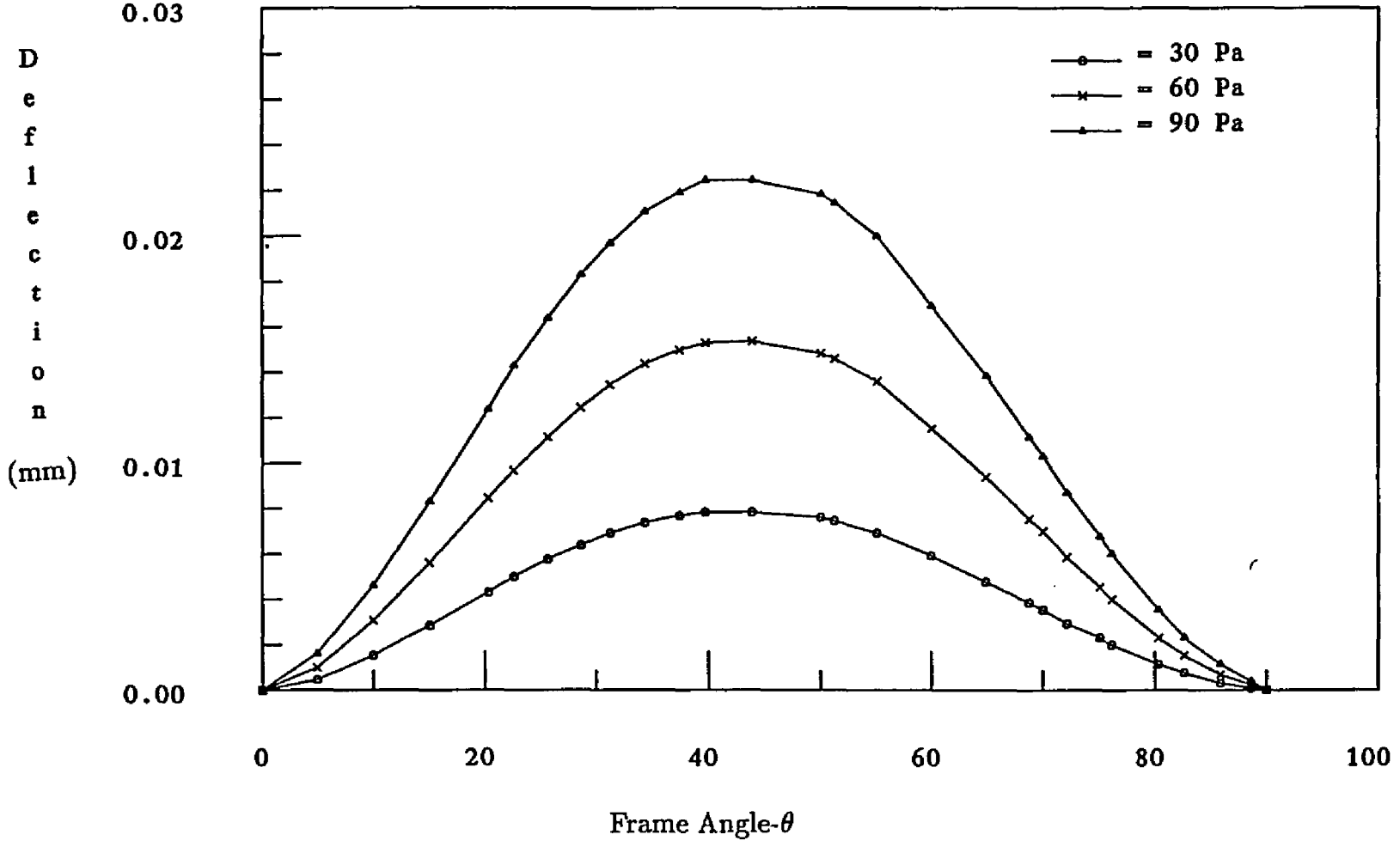

Figure 10. Out-of-Plane Deformation of Frame as a Function of Angular Distance Between the Supports for 2.0-m Dia. Module. (Initial Tension = 16775 N/m, Wind Pressure = 30-90 Pa).

an important design criteria. Based on the maximum permissible deflections, the frame cross section can be redesigned to bring the out-of-plane deflection well within the desired limit.

Figs. 11 and 12 are plotted for the composite membrane out-of-plane deflections at different wind loads from 30-90 Pa. These deflections bear a direct relationship to the focussing requirements of the membrane. It is interesting to note that the deflections show asymmetry. This may be puzzling, but the explanation is straightforward. With the $0^o/60^o/-60^o$ runs of the fibers, the net tensile load on the frame due to the fibers is greater in the y-direction than in the x-direction, as shown in Appendix B. The load asymmetry is causing the deformation asymmetry. With a symmetrical load (i.e. two runs of the fibers at 0^o and 90^o), we expect this asymmetry to disappear.

The load asymmetry is due to the assumption made in the calculation of initial tension. The fiber runs in the directions 0^o, 60^o, and -60^o are perfectly symmetric. And for symmetric runs of fibers, the tension applied is uniform in both directions. It was assumed that when the fibers were equally spaced, adjacent to each other, for the given orientation the fibers crossed and occupied the same point. This would mean that the assumption of equally spaced fibers is not valid. Also, each fiber-resin matrix layer is independently orthotropic. Equivalent material properties for the composite were calculated assuming that the total number of fibers in a given diameter is same, which is not accurate. The error involved in tension computation is given in detail in Appendix D.

As there are no prior load-deformation response studies of the composite membrane, it was difficult to compare the results obtained in this research. There are many analytical solutions available for isotropic membranes, with different support conditions. Also, the work done at SERI [6-8], relates to single and double membranes without the fishnet backing included in this research.

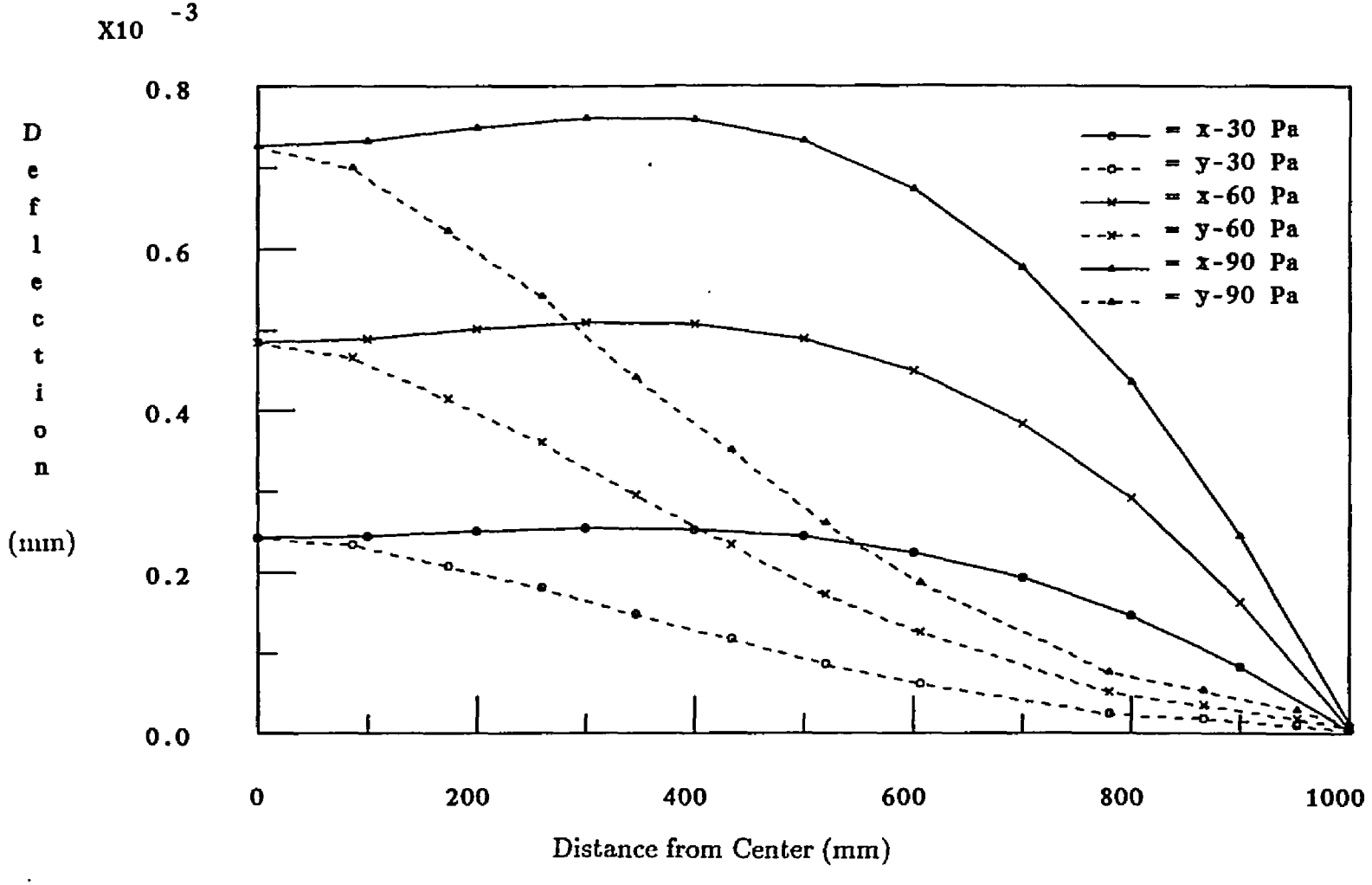

Figure 11. Out-of-Plane Deformation of Membrane as a Function of Radial Distance from the center for 0.2-m Dia. Module. (Initial Tension = 1677.5 N/m, Wind Pressure = 30-90 Pa).

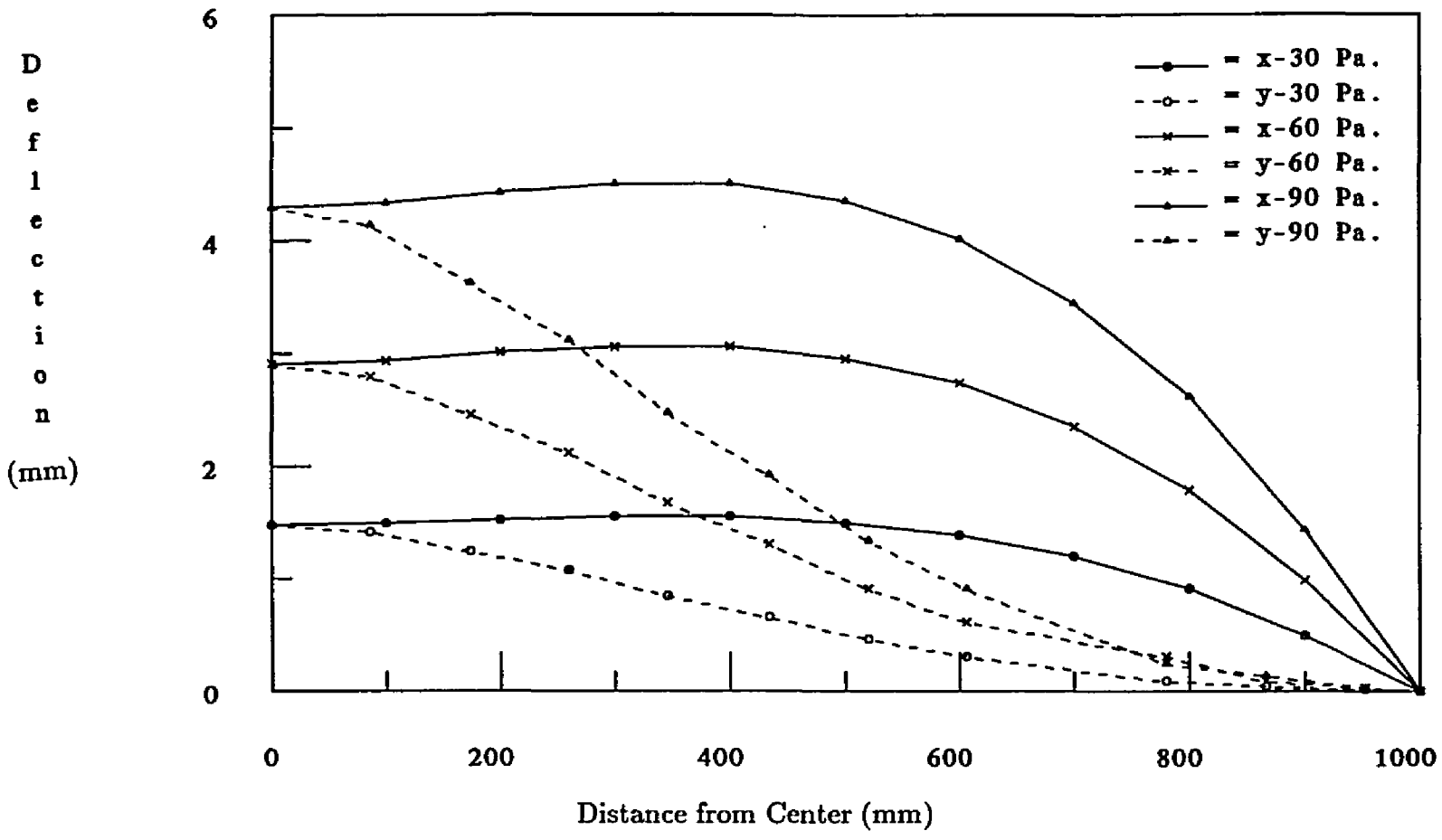

Figure 12. Out-of-Plane Deformation of Membrane as a Function of Radial Distance from the center for 2.0-m Dia. Module. (Initial Tension = 16775 N/m, Wind Pressure = 30-90 Pa).

Discussion

The results give an indication of the load-deformation response of stretched double-membrane solar reflector modules. These results have a direct implication on the surface optical requirements in this specific application. The results throw some light on the design implications and limitations. It also presents a scope for further research in this field.

The results obtained are for 0.2-m, 1.2-m, and 2-m diameter with 10-mm fiber spacing and 2-m diameter module with 25 mm fiber spacing, for wind loads of 30-90 Pa. The results are summarized in Table 4.1.

The difference between 10-mm and 25-mm fiber spacings resulted in changes in initial tension values. The initial tension for the latter case is lower. The deflections for 25-mm spacing is higher than for the 10-mm fiber spacing cases, as the density of the fiber-composite matrix is lower in the 25-mm fiber spacing and hence, less stiff. Also, since the tension is lower for 25-mm fiber spacing, the deflections are high. This clearly supports the concept of initially-stressed membrane, and proves that the deflections vary with the tension. Higher tension yields lower deflection, and vice versa.

Three runs of fibers at the present orientation of $0^o/60^o/\text{-}60^o$ were tried. When extending this concept to larger modules of 11-m and 15-m diameter, a quick estimate of the deflections would help to determine the number of fiber runs.

The fiber material was based on the strength requirements. Though only graphite fibers have been used for the analysis in this research, stainless steel is another choice. Only one thickness of the fibers was used in this analysis. When using other materials such as stainless steel wire (piano wire), the fiber thickness can still be optimized based on the ultimate tensile strength of the material under consideration.

Table 4.1

A Summary of Principal Findings in NASTRAN Analyses of Flat and Curved Reflctors

S. No.	Type	Dia. of Module (m)	Fibers*	Initial Tension in Membrane (N/m)	Wind Load (Pa)	Deflections(mm) Frame Inplane	Frame Out of Plane	Membrane Out of Plane
1	Flat	0.2	0°/ 60°/ -60°	1677.5	30	4.488E-6	3.827E-5	2.540E-4
					60	8.975E-6	7.655E-5	5.058E-4
					90	1.157E-5	1.148E-4	7.619E-4
2	Flat	2.0	"	6710.0	30	4.498E-3	3.233E-2	2.898
					60	5.711E-3	3.966E-2	5.589
					90	7.405E-3	4.636E-2	8.002
3	Flat	2.0	"	16775	30	5.600E-4	7.884E-3	1.549
					60	1.870E-3	1.536E-2	3.062
					90	4.016E-3	2.249E-2	4.512
4	Flat	1.2	"	10065	30	1.010E-4	1.082E-3	0.331
					60	2.034E-4	2.152E-3	0.662
					90	3.119E-4	3.212E-3	0.993
5	Curved	2.0	Radial and Circum-ferential	6710.0	30	6.682E-3	2.125E-2	9.870E-2
					60	1.305E-2	4.245E-2	1.866E-1
					90	1.909E-2	6.365E-2	2.676E-1

* Graphite–Polyimide

The reflective film used here, ECP-91, is 76μm thick. However, ECP-244, which is thicker than the ECP-91, was used in the experimantal construction.

The other parameters which need to be carefully examined are the frame cross section, which affects the membrane out-of-plane deformation, and the membrane attachment to the frame.

CHAPTER 5

COST ANALYSIS

A preliminary cost analysis is shown here. Conservative numbers were used. The costs for the raw materials are from the manufacturers.

The principal assumptions or, more accurately, input parameters are as follows:

The polymer membrane costs $\$0.3/ft^2$. The metallized reflector polymer membrane will be available in bulk in the range of $\$0.4\text{-}0.6/ft^2$, so $\$0.5/ft^2$ has been used. The luan wooden ring for the 2-m diameter size costs \$14.00; weather proofing the ring costs another \$7.00. The labor costs were taken as approximately equal to the material cost, i.e. \$21.00. Thus, the ring costs \$42.00. The selling price was assumed as \$63.00. This translates to $\$1.86/ft^2$. It is assumed that for larger sizes (11m) the costs for the ring will be 80% of the cost per ft^2 for the 2-m diameter, or $\$1.46/ft^2$ of finished reflector area.

Two possible fishnet materials were considered. Stainless steel piano wire (0.015-in. diameter) tensioned to 50-60 kpsi costs \$75.00/16000 ft. The cost of graphite, magnamite AS-4 was \$28.00/10200 ft, or \$30.00/10000 ft in 1984. The three-direction weave ($0°/60°/-60°$) was spaced at 12.5 mm for stainless steel and 10.0 mm for graphite.

A steel ring, in comparison, costs \$51.33 for the 2-m diameter. The labor needed is \$116.00, for a total cost of \$166.00. This leads to $\$3.00/ft^2$ of finished reflector area.

For small quantities, one to ten units, costs are given in Table 5.1, and the costs for mass production are shown in Table 5.2.

Table 5.1

Cost Estimates for Small Number of Modules (in dollars)

		Steel Ring	Wood Ring
a. 2-Meter Diameter.			
Graphite Fiber Fishnet	Membrane	37.20	37.20
	Ring	101.45	62.90
	Fiber	15.17	15.17
	Total	153.82	115.27
	Cost per ft^2	4.55	3.41
Stainless Steel Wire	Membrane	37.20	37.20
	Ring	101.45	62.90
	Fiber	30.12	30.12
	Total	168.77	130.22
	Cost per ft^2	4.99	3.85
a. 11-Meter Diameter.			
Graphite Fiber Fishnet	Membrane	1125.20	1125.20
	Ring	3068.79	1522.12
	Fiber	458.87	454.87
	Total	4648.86	3102.19
	Cost per ft^2	4.54	3.03
Stainless Steel Wire	Membrane	1125.20	1125.20
	Ring	3068.70	1522.12
	Fiber	902.65	902.65
	Total	5096.64	3549.97
	Cost per ft^2	4.99	3.47

Table 5.2

Stressed-Membrane Heliostat Installed at Customer Site
(cost vs. size in 1985 $, 50000 units/year, 1st Units Produced)

	11-m Diameter (Area = 95 m^2)		14-m Diameter (Area = 154 m^2)		20-m Diameter (Area = 314 m^2)	
	Cost	Cost/m^2	Cost	Cost/m^2	Cost	Cost/m^2
Mirror & Support Structure						
Materials	3,046.59	32.07	5,453.53	35.41	13,341.86	42.49
Labor	501.66	5.28	604.58	3.93	725.50	2.31
Equipment (including interest)	122.03	1.28	152.54	0.99	213.56	0.68
Consumables	19.94	0.21	19.94	0.13	28.26	0.09
Total	3,690.22	38.84	6,230.59	40.46	14,309.18	45.57
Drive and Pedestal						
Drive assembly	1,810.00	19.05	1,650.00	10.71	2,847.00	9.07
Pedestal	212.00	2.23	266.00	1.74	500.00	1.59
Assembly drive/pedestal/electric	107.00	1.13	107.00	0.69	107.00	0.34
Total	2,129.00	22.41	2,023.00	13.14	3,454.00	11.00
Foundation	614.00	6.46	934.00	6.06	1,600.00	5.09
Labor (field site)	250.83	2.64	302.29	1.96	500.00	1.59
Buildings (including interest)	13.56	0.14	16.95	0.11	30.00	0.10
Field wiring	434.00	4.57	434.00	2.82	434.00	1.38
Total heliostat cost	7,131.61	75.07	9,940.83	64.55	20,327.66	64.73
DOE & taxes @ 20%	1,426.32	15.01	1,988.16	12.91	465.53	12.95
Selling Price	8,557.93	90.08	11,929.00	77.46	24,393.19	77.68
Present value of 30 yr. O& M	1,545.00	16.26	1,900.00	12.34	2,500.00	7.96
Present value of heliostat and O& M cost	10,102.93	106.34	13,829.00	89.80	26,893.00	85.64

CHAPTER 6

SUMMARY AND CONCLUSION

Summary

The work reported here describes an innovative design for composite structures. The immediate application was to a heliostat; a modified design allows for parabolic dish concentrators. The fundamental principle of utilizing materials near their ultimate strengths resulted in the choice of simple tension members. An inexpensive polymer reflective film membrane stretched over a ring frame was backed by a taut fishnet for stiffness. The load-deformation analyses include the initial tensions and normal wind loads. The ring is supported in a simple manner over a number of equidistant attachment points. In-plane and out-of-plane deformations were calculated for a number of parametric variations that include material choices, fiber spacing, directions of runs, and the frame cross sections. Initial tension and the wind magnitude are the load variations.

The composite structure was analyzed using NASTRAN. Deformations in all three directions were obtained. The numbers compare favorably with previous calculations on similar modules, although the present composite membrane is breaking new ground, rendering the precise comparison difficult. It is seen that the present design offers advantages over not only the conventional glass-metal heliostats, but also the more modern stressed-membrane designs [1, 6]. The code is now being used for extensive design optimizations to construct large modules. Table 4.1 summarizes principal findings of NASTRAN analyses of flat reflectors.

Experimental modules were constructed using graphite-fiber fishnets and a popular reflective-film membrane. These modules were tested structurally and optically

for solar reflectance performance. While the construction feasibility was demonstrated, a persisting problem is the "print through", where the fibers reveal their presence through the thin stretched membrane. Also, the effect of long-term exposure to weather is needed. These problems are currently being investigated.

This concept was extended to parabolic dish concentrators and two modules were fabricated in a similar manner. The fabrication process is described in Appendix C. The "print through" problem persisted and is being solved by trying different forms of fiber materials such as woven cloth and also inserting a foam layer between the film and fibers.

In addition, the easy adaption to industry production is being aided by one of the manufacturers.

A first-cut cost analysis was developed. It was found that both in small numbers and in mass production the costs are likely to be low.

In summary, it was found through quantitative calculations and actual experimental fabrications that the innovation of advanced high-tech composites can greatly facilitate the acceptability of this energy technology.

Conclusion

Both flat and curved (parabolic and spherical) reflectors were built, modelled, and analyzed. The progress made is a clear indication of the realistic promise of this new and innovative technology.

There are some principal issues still to be solved in this design of reflector modules with advanced composites, especially when the application calls for a high-quality optical surface. The minor problems, membrane attachment and interactions with the frame, aging under stressed conditions, fiber "print through", resin

and fiber loading, and membrane wrinkling, can nevertheless be solved. For example, the resin loading is of interest to all applications of composites materials. Some of these specific issues need immediate attention and are discussed below.

First are membrane distortions, which include large scale "waviness" and small scale "wrinkling". These cause focussing errors and collector inefficiencies, and could result in accidental overheating. It was discovered during the fabrication process that small variations in the ring-membrane attachment can start a distortion. These distortions quickly spread and amplify the "waviness" and "wrinkles" on the membranes. The ring frame may thus have to be much stiffer than the simple deflection limits suggested by the analytical solutions. However, this can be investigated using a computer model. Also, the membrane tension, which induces a compressive stress in the frame, needs to be optimized along with the frame design. These interact and must be solved iteratively.

The "print through" problem was a persistent one. This is accounted for as follows. During resin curing, a differential stress is introduced. This, and differences in the thermal expansion coefficients of the membrane and the fiber-resin composite, as well as the thickness of the membrane, may cause the fibers to "print through" as seen during the fabrication process. This issue needs to be addressed with caution, as any compromise in the thickness of the membrane or the fiber-resin composite could undermine the fundamental objective of achieving low-cost and low-weight design.

The other problems mentioned above are solved easily with some research, literature surveys and studies. They are not discussed here as they are beyond the scope of this present research.

The value of the analytical solutions in the present context can not be overemphasized. They offer a greater insight and flexibilty than the numerical solutions.

In general, considering the nonlinearity of the problem, success may be limited in getting a converged solution. So, we considered numerical methods as an alternative solution to our problem. The most straightforward approach is with a general nonlinear finite-element analysis. Though certainly quite general, the finite-element approach is expensive and cumbersome, and often simple relationships are difficult to glean from them. This approach needs to be planned carefully to make full use of both computer's and researcher's time. Therefore, the most important aspect of this work is the success through proper convergence of the solutions. Nevertheless, the results obtained in this research will greatly aid the widespread use of solar reflectors with advanced-composite technology.

This new and innovative design promises a bright future for advanced composites in applications where cost and weight are important considerations without sacrificing on strength, efficiency, and performance.

APPENDIX A

INPUT DATA FOR NASTRAN

- The quarter model was generated using GIFTS as an interface.
- Triangular membrane elements for composite layup of polymer film and graphite fibers were used. At some places, quadrilateral elements were necessary.
- Frame made of wood, with a cross section of 63.5 × 35.56 mm was used.
- Solid elements were used for circular ring frame.
- Nonlinear solution Type 64 was used in NASTRAN.
- Material Properties used were:

  –Wood[1]–Oak was assumed.

  E = Young's Modulus = 2.11×10^6 psi = 1483.826 kg/mm^2

  μ = Poisson's Ratio = 0.3 (assumed)

  G = Bulk Modulus = E/[2(1 + μ)] = 570.70 kg/mm^2

  ρ = Density = 46 lb/ft^3 = 7.3686×10^{-6} kg/mm^3

  –Polymer (Membrane) Film[2] – ECP–91

  Thickness = 0.076 mm (76μm)

  E = Young's Modulus = 550,000 psi = 3.8678×10^2 kg/mm^2

  μ = Poisson's Ratio = 0.4

  G = Bulk Modulus = E/[2(1 + μ)] = 1.3814×10^2 kg/mm^2

  ρ = Density = 1.497×10^{-6} kg/mm^3

---

[1] Handbook of Industrial Materials, pp 320.

[2] Personal Communication from Mr. John Roach, 3M Company, Minnesota.

The following data are mandatory for NASTRAN input deck. They have been assumed for that purpose, although they may not be relevant for the computation of deflection in this specific analysis.

$G_{1,z}$ = Trans. Shear Modulus = 1.6174×10^2 kg/mm^2 (1–z plane)

$G_{2,z}$ = Trans. Shear Modulus = 1.6174×10^2 kg/mm^2 (2–z plane)

A_1 = Thermal Expansion Coefficient = 10×10^{-6} mm/mm/°F

A_2 = Thermal Expansion Coefficient = 5×10^{-6} mm/mm/°F

T_{ref} = Reference Temperature for Thermal Expansion = 32°F

x_t,x_c = Allowable Stresses in Tension and Compression = 100 kg/mm^2

y_t,y_c = Allowable Stresses in Tension and Compression = 100 kg/mm^2

S = Allowable Stress for In-plane Shear = 7.74 kg/mm^2

GE = Structural Damping Coefficient = 1.0×10^{-4}

–Graphite Fibers[3]

E_1 = Long. Young's Modulus = 34×10^6 psi = 2.391×10^4 kg/mm^2

E_2 = Trans. Young's Modulus = 1×10^6 psi = 7.0323×10^4 kg/mm^2

μ_{12} = Poisson's Ratio in 1–2 direction = 0.25 (assumed)

G_{12} = Bulk Modulus 1–2 direction = 3.4×10^6 psi = 2.391×10^3 kg/mm^2

ρ = 0.65 lb/in^3 = 1.80×10^{-6} kg/mm^2

–Polyimide Resin[4]

E_1 = Long. Young's Modulus = 5.6×10^5 psi = 3.938×10^2 kg/mm^2

E_2 = Trans. Young's Modulus = 5.6×10^5 psi = 3.938×10^2 kg/mm^2

μ_{12} = Poisson's Ratio in 1–2 direction = 0.35 (assumed)

---

[3] Magnamite Graphite Type AS–4, Hercules Product.

[4] Handbook of Industrial Materials, pp 434.

G_{12} = Bulk Modulus 1–2 direction = 2.4×10^5 psi = 1.688×10^2 kg/mm^2

$\rho = 2 \times \rho$ of epoxy resin (assumed)

The Density of polyimide resin was calculated as follows:[5]

Density of fiber alone = 0.074 lb/in^3

Density of fiber-epoxy composite = 0.061 lb/in^3

Fiber volume fraction = 55% = 0.55

By rule of mixtures:

$$\rho_c = \rho_f V_f + \rho_m V_m$$

$\rho_c = 0.061$, $\rho_f = 0.074$, $V_f = 0.55$, $V_m = 0.45$

Substituting these values in the above equation,

$0.061 = 0.074 \times 0.55 + \rho_m \times 0.45$

Therefore, $\rho_m = 0.045$ lb/in^3 (for epoxy)

Again, from assumption that the density of polyimide is twice that of epoxy,

Density of polyimide = $2 \times 0.045 = 0.090$ lb/in^3

Here, ρ_c = Density of composite,

ρ_f = Density of fibers, and

ρ_m = Density of matrix and

V_f, and V_m represent the volume fraction of fibers and matrix, respectively.

Based on the above values, the properties for the graphite fibers-polyimide matrix were calculated assuming a volume fraction of 50%.

$$E_{1c} = E_{1f} V_f + E_{1m} V_m$$
$$= (2.391 \times 10^4 \times 0.5) + (3.9831 \times 10^2 \times 0.5)$$
$$= 1.2152 \times 10^4 \text{ kg/mm}^2$$

---

[5] From Union Carbide Data Sheet.

$$E_{2c} = E_m E_f/(E_f V_m + E_m V_f)$$
$$= 4.7531 \times 10^2$$
$$\mu_{LT1} = 0.25 \times 0.5 + 0.35 \times 0.5 = 0.3$$
$$G_{LT1} = G_m G_f/(G_f V_m + G_m V_f)$$
$$= 3.153 \times 10^2 \text{ kg/mm}^2$$
$$\rho_{LT1} = 2.497 \times 10^{-6} \times 0.5 + 1.80 \times 10^{-6} \times 0.5$$
$$= 2.1482 \times 10^{-6}$$

Refer to Fig. A.1 for the arrangement of layers.

• For the first layer, the properties of polymer film were input directly to the NASTRAN data deck.

• For the subsequent layers of graphite-polyimide matrix, equivalent properties were calculated based on the volume fraction. An imaginary matrix is assumed between adjacent runs of fiber whose properties are taken to be equal to zero.

$$V_f = A_f/A_c \text{ and } V_m = A_m/A_c = 0$$
$$A_f = 3.77 \times 10^{-4} = 0.2432 \text{ mm}^2$$

For 100 fibers along a radius of 1000 mm at a spacing of 10 mm, the total area of fibers is given by, $A_f = 24.32$ mm^2.

• Area of matrix plus fibers = 1000 × diameter of fiber;

$$A_c = 1000 \times 0.5565 = 556.5 \text{ mm}^2$$

For 100 fibers,

$$V_f = A_f/A_c = 24.32/556.5 = 0.0437$$

Therefore,

$$E_{1c} = 1.2152 \times 10^4 \times 0.0437 = 5.3114 \times 10^2 \text{ kg/mm}^2$$
$$E_{2c} = 23.97 \text{ kg/mm}^2$$
$$\rho_{LTc} = 0.3 \times 0.0437 = 0.01311$$
$$G_{LTc} = 2.6213 \times 10^2 \text{ kg/mm}^2$$
$$\rho_{LTc} = 2.2493 \times 10^{-6} \times 0.0437 = 9.8308 \times 10^{-8}$$

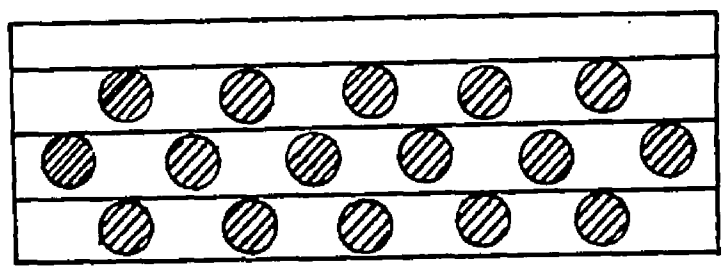

	Orientation
ECP-91	0°
Graphite	0°
Graphite	60°
Graphite	-60°

Figure A.1 Composite Layer Arrangement for NASTRAN Input

Model Generation

The model for the finite element analysis was generated using GIFTS, finite element package. First, the boundary of the model was defined. Then suitable grids were defined for element generation. The elements were chosen based on the problem type. Since, the problem considered required membrane analysis, triangular and quadrilateral membrane elements were chosen for the composite membrane. For the frame, eight-noded solid elements were chosen. Once the boundary is defined, the GIFTS program is capable of generating nodes and elements automatically. The model was drawn on a graphics screen and the correctness of the model was verified. Loads and boundary conditions were input. The nodes and elements were renumbered using GIFTS optimization routine. The optimization was done to reduce the bandwidth, since the band-width and the number of unknowns, relates to the solution time of the model.

NASTRAN input data deck from GIFTS data base was created using an interface routine, GFTMSC. This deck creates the case control and the bulk data decks for the NASTRAN run. The executive control deck was added to the above data file. For the analysis of composite structures, PCOMP cards were added.

This data file was run in batch process to obtain the results. The job was rerun, if necessary, until the solution converged.

A sample input data file for a NASTRAN job, is given in the following pages.

```
ID MODEL5 NASTRAN
SOL 64
TIME 20
CEND
 TITLE = 0.2 meter DIA MODULE : TREATED AS COMPOSITE LAYUP
 SUBTITLE = 10 mm SPACING BETWEEN FIBERS - GRAPHITE - p = 30 pascals
 OUTPUT
    LOAD = 1
    DISP = ALL
 SUBCASE 1
    LABEL = linear static solution
 SUBCASE 2
    LABEL = differential stiffness solution
 SUBCASE 3
    LABEL = I NON-LINEAR SOLUTION
 SUBCASE 4
    LABEL = II NON-LINEAR SOLUTION
    PARAM,SKIPMTRX,-1
 SUBCASE 5
    LABEL = III NON LINEAR SOLUTION
 SUBCASE 6
    LABEL = IV NON LINEAR SOLUTION
    PARAM,SKIPMTRX,1
BEGIN BULK
param,autospc,yes
param,testneg,-2
pload2,1,-3.058-6,1 thru 200
mat8,1,3.8678+2,4.2194+2,0.40,1.3814+2,1.6174+2,1.6174+2,1.497-6,abc
+bc,20.-6,10.-6,32.,1.+2,1.+2,1.+2,1.+2,7.74,def
+ef,1.-4
mat8,2,5.3114+2,23.974,.01312,2.6213+2,53.114,23.974,9.3754-8,ghj
+hj,10.-6,5.-6,32.,1.+2,1.+2,1.+2,1.+2,53.114,klm
+lm,1.-4
pcomp,1,-.87275,0.0,4.22,,32.,1.-4,,nop
+op,1,0.076,0.,no,2,.5565,0.,no,qrs
+rs,2,.5565,60.,no,2,.5565,-60.,no
pcomp,2,-.87275,0.0,4.22,,32.,1.-4,,tuv
+uv,2,.5565,-60.,no,2,.5565,60.,no,wxy
+xy,2,.5565,0.0,no,1,0.076,0.0,no
GRID     1       0       110.16000.      6.3500000       123456
GRID     2       0       100.00000.      6.3500000       2456
GRID     3       0       99.630008.6600006.3500000       456
GRID     4       0       109.81908.6600006.3500000       456
GRID     5       0       100.00000.      -6.350000       2456
GRID     6       0       110.16000.      -6.350000       123456
GRID     7       0       99.630008.660000-6.350000       456
GRID     8       0       109.81908.660000-6.350000       456
GRID     9       0       90.000000.      6.3500000       2456
GRID     10      0       95.000008.6599996.3500000       456
GRID     11      0       98.4920017.320016.3500000       456
GRID     12      0       108.789017.320016.3500000       456
GRID     13      0       98.4920017.32001-6.350000       456
GRID     14      0       108.789017.32001-6.350000       456
GRID     15      0       90.000000.      -6.350000       2456
GRID     16      0       95.000008.659999-6.350000       456
GRID     17      0       80.000000.      6.3500000       2456
GRID     18      0       85.000008.6599996.3500000       456
GRID     19      0       90.0000017.319996.3500000       456
GRID     20      0       96.5659925.980006.3500000       456
GRID     21      0       107.052025.980006.3500000       456
GRID     22      0       96.5659925.98000-6.350000       456
GRID     23      0       107.052025.98000-6.350000       456
GRID     24      0       90.0000017.31999-6.350000       456
GRID     25      0       80.000000.      -6.350000       2456
GRID     26      0       85.000008.659999-6.350000       456
GRID     27      0       70.000000.      6.3500000       2456
GRID     28      0       75.000008.6599996.3500000       456
```

```
GRID     29        0       80.0000217.320026.3500000       456
GRID     30        0       85.0000025.980006.3500000       456
GRID     31        0       91.6908034.640406.3500000       456
GRID     32        0       93.8233934.641016.3500000       456
GRID     33        0       104.572034.640006.3500000       456
GRID     34        0       93.8233934.64101-6.350000       456
GRID     35        0       104.572034.64000-6.350000       456
GRID     36        0       85.0000025.98000-6.350000       456
GRID     37        0       91.6908034.64040-6.350000       456
GRID     38        0       80.0000217.32002-6.350000       456
GRID     39        0       70.000000.      -6.350000       2456
GRID     40        0       75.000008.659999-6.350000       456
GRID     41        0       60.000000.      6.3500000       2456
GRID     42        0       65.000008.6599996.3500000       456
GRID     43        0       70.0000017.320076.3500000       456
GRID     44        0       75.0000025.980076.3500000       456
GRID     45        0       80.0000034.640406.3500000       456
GRID     46        0       86.8156043.300806.3500000       456
GRID     47        0       92.2650038.564006.3500000       456
GRID     48        0       90.1400043.360996.3500000       456
GRID     49        0       101.290043.300006.3500000       456
GRID     50        0       92.2650038.56400-6.350000       456
GRID     51        0       101.290043.30000-6.350000       456
GRID     52        0       80.0000034.64040-6.350000       456
GRID     53        0       75.0000025.98007-6.350000       456
GRID     54        0       86.8156043.30080-6.350000       456
GRID     55        0       90.1400043.36099-6.350000       456
GRID     56        0       70.0000017.32007-6.350000       456
GRID     57        0       60.000000.      -6.350000       2456
GRID     58        0       65.000008.659999-6.350000       456
GRID     59        0       50.000000.      6.3500000       2456
GRID     60        0       55.000008.6599996.3500000       456
GRID     61        0       59.9999817.320106.3500000       456
GRID     62        0       65.0000025.980156.3500000       456
GRID     63        0       70.0000034.640466.3500000       456
GRID     64        0       75.0000043.300806.3500000       456
GRID     65        0       81.9404051.961206.3500000       456
GRID     66        0       87.7200048.013006.3500000       456
GRID     67        0       85.4780051.962016.3500000       456
GRID     68        0       98.4900149.345996.3500000       456
GRID     69        0       98.4900149.34599-6.350000       456
GRID     70        0       97.1360051.960016.3500000       456
GRID     71        0       87.7200048.01300-6.350000       456
GRID     72        0       97.1360051.96001-6.350000       456
GRID     73        0       75.0000043.30080-6.350000       456
GRID     74        0       70.0000034.64046-6.350000       456
GRID     75        0       65.0000025.98015-6.350000       456
GRID     76        0       81.9404051.96120-6.350000       456
GRID     77        0       85.4780051.96201-6.350000       456
GRID     78        0       59.9999817.32010-6.350000       456
GRID     79        0       50.000000.      -6.350000       2456
GRID     80        0       55.000008.659999-6.350000       456
GRID     81        0       40.000000.      6.3500000       2456
GRID     82        0       45.000008.6600006.3500000       456
GRID     83        0       50.0000017.320136.3500000       456
GRID     84        0       54.9999825.980226.3500000       456
GRID     85        0       59.9999834.640526.3500000       456
GRID     86        0       65.0000243.300846.3500000       456
GRID     87        0       70.0000051.961206.3500000       456
GRID     88        0       77.0652060.621606.3500000       456
GRID     89        0       82.5690056.412006.3500000       456
GRID     90        0       79.5470060.621996.3500000       456
GRID     91        0       93.5679958.141016.3500000       456
GRID     92        0       93.5679958.14101-6.350000       456
GRID     93        0       91.9810060.621996.3500000       456
GRID     94        0       82.5690056.41200-6.350000       456
GRID     95        0       91.9810060.62199-6.350000       456
```

```
GRID    96      0       70.0000051.96120-6.350000       456
GRID    97      0       65.0000243.30084-6.350000       456
GRID    98      0       59.9999834.64052-6.350000       456
GRID    99      0       54.9999825.98022-6.350000       456
GRID    100     0       77.0652060.62160-6.350000       456
GRID    101     0       79.5470060.62199-6.350000       456
GRID    102     0       50.0000017.32013-6.350000       456
GRID    103     0       40.000000.      -6.350000       2456
GRID    104     0       45.000008.660000-6.350000       456
GRID    105     0       30.000000.      6.3500000       2456
GRID    106     0       35.000008.6600006.3500000       456
GRID    107     0       40.0000217.320166.3500000       456
GRID    108     0       45.0000025.980296.3500000       456
GRID    109     0       50.0000234.640586.3500000       456
GRID    110     0       55.0000043.300896.3500000       456
GRID    111     0       60.0000051.961216.3500000       456
GRID    112     0       65.0000060.621606.3500000       456
GRID    113     0       72.1900069.282006.3500000       456
GRID    114     0       76.9040163.920006.3500000       456
GRID    115     0       88.1463066.072016.3500000       456
GRID    116     0       88.1463066.07201-6.350000       456
GRID    117     0       85.6499969.280006.3500000       456
GRID    118     0       76.9040163.92000-6.350000       456
GRID    119     0       85.6499969.28000-6.350000       456
GRID    120     0       65.0000060.62160-6.350000       456
GRID    121     0       60.0000051.96121-6.350000       456
GRID    122     0       55.0000043.30089-6.350000       456
GRID    123     0       50.0000234.64058-6.350000       456
GRID    124     0       45.0000025.98029-6.350000       456
GRID    125     0       72.1900069.28200-6.350000       456
GRID    126     0       40.0000217.32016-6.350000       456
GRID    127     0       30.000000.      -6.350000       2456
GRID    128     0       35.000008.660000-6.350000       456
GRID    129     0       20.000000.      6.3500000       2456
GRID    130     0       25.000008.6600006.3500000       456
GRID    131     0       30.0000017.320196.3500000       456
GRID    132     0       35.0000025.980366.3500000       456
GRID    133     0       40.0000034.640646.3500000       456
GRID    134     0       45.0000043.300926.3500000       456
GRID    135     0       50.0000051.961236.3500000       456
GRID    136     0       55.0000060.621576.3500000       456
GRID    137     0       60.0000069.282006.3500000       456
GRID    138     0       64.2440076.633006.3500000       456
GRID    139     0       82.2899973.241006.3500000       456
GRID    140     0       82.2899973.24100-6.350000       456
GRID    141     0       72.1180083.272006.3500000       456
GRID    142     0       64.2440076.63300-6.350000       456
GRID    143     0       72.1180083.27200-6.350000       456
GRID    144     0       60.0000069.28200-6.350000       456
GRID    145     0       55.0000060.62157-6.350000       456
GRID    146     0       50.0000051.96123-6.350000       456
GRID    147     0       45.0000043.30092-6.350000       456
GRID    148     0       40.0000034.64064-6.350000       456
GRID    149     0       35.0000025.98036-6.350000       456
GRID    150     0       30.0000017.32019-6.350000       456
GRID    151     0       20.000000.      -6.350000       2456
GRID    152     0       25.000008.660000-6.350000       456
GRID    153     0       10.000000.      6.3500000       2456
GRID    154     0       15.000008.6600006.3500000       456
GRID    155     0       20.0000017.320246.3500000       456
GRID    156     0       25.0000025.980446.3500000       456
GRID    157     0       30.0000034.640706.3500000       456
GRID    158     0       35.0000043.300966.3500000       456
GRID    159     0       40.0000051.961246.3500000       456
GRID    160     0       45.0000060.621546.3500000       456
GRID    161     0       50.0000069.281886.3500000       456
GRID    162     0       55.0000077.941016.3500000       456
```

```
GRID    163     0       62.7000077.942006.3500000       456
GRID    164     0       68.0860086.603006.3500000       456
GRID    165     0       62.7000077.94200-6.350000       456
GRID    166     0       68.0860086.60300-6.350000       456
GRID    167     0       55.0000077.94101-6.350000       456
GRID    168     0       50.0000069.28188-6.350000       456
GRID    169     0       45.0000060.62154-6.350000       456
GRID    170     0       40.0000051.96124-6.350000       456
GRID    171     0       35.0000043.30096-6.350000       456
GRID    172     0       30.0000034.64070-6.350000       456
GRID    173     0       25.0000025.98044-6.350000       456
GRID    174     0       20.0000017.32024-6.350000       456
GRID    175     0       10.000000.      -6.350000       2456
GRID    176     0       15.000008.660000-6.350000       456
GRID    177     0       0.      0.      6.3500000       12456
GRID    178     0       5.0000008.6600006.3500000       456
GRID    179     0       10.0000017.320276.3500000       456
GRID    180     0       15.0000025.980516.3500000       456
GRID    181     0       20.0000034.640766.3500000       456
GRID    182     0       25.0000043.301016.3500000       456
GRID    183     0       30.0000051.961266.3500000       456
GRID    184     0       35.0000060.621516.3500000       456
GRID    185     0       40.0000069.281756.3500000       456
GRID    186     0       45.0000077.942006.3500000       456
GRID    187     0       50.0000086.600016.3500000       456
GRID    188     0       57.3210081.947016.3500000       456
GRID    189     0       63.1400090.270006.3500000       456
GRID    190     0       57.3210081.94701-6.350000       456
GRID    191     0       63.1400090.27000-6.350000       456
GRID    192     0       45.0000077.94200-6.350000       456
GRID    193     0       50.0000086.60001-6.350000       456
GRID    194     0       40.0000069.28175-6.350000       456
GRID    195     0       35.0000060.62151-6.350000       456
GRID    196     0       30.0000051.96126-6.350000       456
GRID    197     0       25.0000043.30101-6.350000       456
GRID    198     0       20.0000034.64076-6.350000       456
GRID    199     0       15.0000025.98051-6.350000       456
GRID    200     0       10.0000017.32027-6.350000       456
GRID    201     0       0.      0.      -6.350000       12456
GRID    202     0       5.0000008.660000-6.350000       456
GRID    203     0       0.      8.6600006.3500000       1456
GRID    204     0       0.      17.320016.3500000       1456
GRID    205     0       5.00000025.981006.3500000       456
GRID    206     0       10.0000034.641146.3500000       456
GRID    207     0       15.0000043.301326.3500000       456
GRID    208     0       20.0000051.961496.3500000       456
GRID    209     0       25.0000060.621666.3500000       456
GRID    210     0       30.0000069.281836.3500000       456
GRID    211     0       35.0000077.942006.3500000       456
GRID    212     0       40.0000086.603006.3500000       456
GRID    213     0       42.3220190.603006.3500000       456
GRID    214     0       55.3000095.000006.3500000       456
GRID    215     0       55.3000095.00000-6.350000       456
GRID    216     0       47.4299998.837016.3500000       456
GRID    217     0       42.3220190.60300-6.350000       456
GRID    218     0       47.4299998.83701-6.350000       456
GRID    219     0       35.0000077.94200-6.350000       456
GRID    220     0       40.0000086.60300-6.350000       456
GRID    221     0       30.0000069.28183-6.350000       456
GRID    222     0       25.0000060.62166-6.350000       456
GRID    223     0       20.0000051.96149-6.350000       456
GRID    224     0       15.0000043.30132-6.350000       456
GRID    225     0       10.0000034.64114-6.350000       456
GRID    226     0       5.00000025.98100-6.350000       456
GRID    227     0       0.      17.32001-6.350000       1456
GRID    228     0       0.      8.660000-6.350000       1456
GRID    229     0       0.      25.981006.3500000       1456
```

```
GRID     230       0          0.      34.640006.3500000        1456
GRID     231       0          5.00000043.360996.3500000         456
GRID     232       0          10.0000052.009376.3500000         456
GRID     233       0          15.0000060.657786.3500000         456
GRID     234       0          20.0000069.306186.3500000         456
GRID     235       0          25.0000077.954596.3500000         456
GRID     236       0          30.0000086.603006.3500000         456
GRID     237       0          36.1750093.227016.3500000         456
GRID     238       0          34.2640193.947016.3500000         456
GRID     239       0          44.97400100.00006.3500000         456
GRID     240       0          36.1750093.22701-6.350000         456
GRID     241       0          44.97400100.0000-6.350000         456
GRID     242       0          25.0000077.95459-6.350000         456
GRID     243       0          30.0000086.60300-6.350000         456
GRID     244       0          34.2640193.94701-6.350000         456
GRID     245       0          20.0000069.30618-6.350000         456
GRID     246       0          15.0000060.65778-6.350000         456
GRID     247       0          10.0000052.00937-6.350000         456
GRID     248       0          5.00000043.36099-6.350000         456
GRID     249       0          0.      34.64000-6.350000         1456
GRID     250       0          0.      25.98100-6.350000         1456
GRID     251       0          0.      43.360996.3500000         1456
GRID     252       0          0.      51.962016.3500000         1456
GRID     253       0          5.00000060.621996.3500000         456
GRID     254       0          10.0000069.282326.3500000         456
GRID     255       0          15.0000077.942666.3500000         456
GRID     256       0          20.0000086.603006.3500000         456
GRID     257       0          25.0000095.263006.3500000         456
GRID     258       0          30.6100095.263006.3500000         456
GRID     259       0          39.35400102.87006.3500000         456
GRID     260       0          39.35400102.8700-6.350000         456
GRID     261       0          35.69000104.06006.3500000         456
GRID     262       0          30.6100095.26300-6.350000         456
GRID     263       0          35.69000104.0600-6.350000         456
GRID     264       0          20.0000086.60300-6.350000         456
GRID     265       0          15.0000077.94266-6.350000         456
GRID     266       0          25.0000095.26300-6.350000         456
GRID     267       0          10.0000069.28232-6.350000         456
GRID     268       0          5.00000060.62199-6.350000         456
GRID     269       0          0.      51.96201-6.350000         1456
GRID     270       0          0.      43.36099-6.350000         1456
GRID     271       0          0.      60.621996.3500000         1456
GRID     272       0          0.      69.282006.3500000         1456
GRID     273       0          5.00000077.942326.3500000         456
GRID     274       0          10.0000086.602666.3500000         456
GRID     275       0          15.0000095.263006.3500000         456
GRID     276       0          25.8140096.610996.3500000         456
GRID     277       0          23.9440097.091006.3500000         456
GRID     278       0          16.9470198.552996.3500000         456
GRID     279       0          31.02699105.70006.3500000         456
GRID     280       0          25.8140096.61099-6.350000         456
GRID     281       0          31.02699105.7000-6.350000         456
GRID     282       0          10.0000086.60266-6.350000         456
GRID     283       0          15.0000095.26300-6.350000         456
GRID     284       0          5.00000077.94232-6.350000         456
GRID     285       0          23.9440097.09100-6.350000         456
GRID     286       0          16.9470198.55299-6.350000         456
GRID     287       0          0.      69.28200-6.350000         1456
GRID     288       0          0.      60.62199-6.350000         1456
GRID     289       0          0.      77.942006.3500000         1456
GRID     290       0          0.      86.603006.3500000         1456
GRID     291       0          5.00000095.263006.3500000         456
GRID     292       0          12.7350099.186006.3500000         456
GRID     293       0          7.57100099.713006.3500000         456
GRID     294       0          22.28700107.88206.3500000         456
GRID     295       0          22.28700107.8820-6.350000         456
GRID     296       0          17.17670108.81206.3500000         456
```

```
GRID     297      0        17.17670108.8120-6.350000        456
GRID     298      0        14.51020109.06706.3500000        456
GRID     299      0        12.7350099.18600-6.350000        456
GRID     300      0        14.51020109.0670-6.350000        456
GRID     301      0        0.       86.60300-6.350000       1456
GRID     302      0        5.00000095.26300-6.350000        456
GRID     303      0        7.57100099.71300-6.350000        456
GRID     304      0        0.       77.94200-6.350000       1456
GRID     305      0        0.       95.263006.3500000       1456
GRID     306      0        2.28000099.974006.3500000        456
GRID     307      0        0.       100.00006.3500000       1456
GRID     308      0        9.148000109.99006.3500000        456
GRID     309      0        9.148000109.9900-6.350000        456
GRID     310      0        2.280000110.13206.3500000        456
GRID     311      0        2.28000099.97400-6.350000        456
GRID     312      0        2.280000110.1320-6.350000        456
GRID     313      0        0.       95.26300-6.350000       1456
GRID     314      0        0.       100.0000-6.350000       1456
GRID     315      0        0.       110.16006.3500000       123456
GRID     316      0        0.       110.1600-6.350000       123456
MAT1     3        1483.826570.7000.3000000.7369E-6.6500E-50.       0.
CTRIA3,  1,1,253,272,254, 149.999
CTRIA3,  2,1,273,254,272,  59.999
CTRIA3,  3,1,254,273,255, 149.999
CTRIA3,  4,1,274,255,273,  59.999
CTRIA3,  5,1,255,274,256, 149.999
CTRIA3,  6,1,275,256,274,  59.999
CTRIA3,  7,1,236,235,256, 180.000
CTRIA3,  8,1,256,257,236,  59.999
CTRIA3,  9,1,235,234,255, 180.000
CTRIA3, 10,1,255,256,235,  60.000
CTRIA3, 11,1,234,233,254, 180.000
CTRIA3, 12,1,254,255,234,  60.000
CTRIA3, 13,1,233,232,253, 180.000
CTRIA3, 14,1,253,254,233,  60.000
CTRIA3, 15,1,232,231,252, 180.000
CTRIA3, 16,1,252,253,232,  59.999
CTRIA3, 17,1,211,210,235, 180.000
CTRIA3, 18,1,235,236,211,  59.966
CTRIA3, 19,1,210,209,234, 180.000
CTRIA3, 20,1,234,235,210,  59.966
CTRIA3, 21,1,209,208,233, 180.000
CTRIA3, 22,1,233,234,209,  59.966
CTRIA3, 23,1,208,207,232, 180.000
CTRIA3, 24,1,232,233,208,  59.966
CTRIA3, 25,1,207,206,231, 180.000
CTRIA3, 26,1,231,232,207,  59.966
CTRIA3, 27,1,206,205,230, 180.000
CTRIA3, 28,1,230,231,206,  60.173
CTRIA3, 29,1,186,185,211, 180.000
CTRIA3, 30,1,211,212,186,  60.002
CTRIA3, 31,1,185,184,210, 180.000
CTRIA3, 32,1,210,211,185,  60.000
CTRIA3, 33,1,184,183,209, 180.000
CTRIA3, 34,1,209,210,184,  60.000
CTRIA3, 35,1,183,182,208, 180.000
CTRIA3, 36,1,208,209,183,  60.000
CTRIA3, 37,1,182,181,207, 180.000
CTRIA3, 38,1,207,208,182,  60.000
CTRIA3, 39,1,181,180,206, 180.000
CTRIA3, 40,1,206,207,181,  60.000
CTRIA3, 41,1,180,179,205, 180.000
CTRIA3, 42,1,205,206,180,  60.000
CTRIA3, 43,1,179,178,204, 180.000
CTRIA3, 44,1,204,205,179,  60.002
CTRIA3, 45,1, 30, 20, 31,     .000
CTRIA3, 46,1, 31, 45, 30, 180.000
```

```
CTRIA3, 47,1, 45, 31, 46,    .000
CTRIA3, 48,1, 46, 64, 45, 180.000
CTRIA3, 49,1, 64, 46, 65,    .000
CTRIA3, 50,1, 65, 87, 64, 180.000
CTRIA3, 51,1, 87, 65, 88,    .000
CTRIA3, 52,1, 88,112, 87, 180.000
CTRIA3, 53,1,112, 88,113,    .000
CTRIA3, 54,1,113,137,112, 180.000
CTRIA3, 55,1,177,153,178,    .000
CTRIA3, 56,1,154,178,153, 180.000
CTRIA3, 57,1,153,129,154,    .000
CTRIA3, 58,1,130,154,129, 180.000
CTRIA3, 59,1,129,105,130,    .000
CTRIA3, 60,1,106,130,105, 180.000
CTRIA3, 61,1,105, 81,106,    .000
CTRIA3, 62,1, 82,106, 81, 180.000
CTRIA3, 63,1, 81, 59, 82,    .000
CTRIA3, 64,1, 60, 82, 59, 180.000
CTRIA3, 65,1, 59, 41, 60,    .000
CTRIA3, 66,1, 42, 60, 41, 180.000
CTRIA3, 67,1, 41, 27, 42,    .000
CTRIA3, 68,1, 28, 42, 27, 180.000
CTRIA3, 69,1, 27, 17, 28,    .000
CTRIA3, 70,1, 18, 28, 17, 180.000
CTRIA3, 71,1, 17,  9, 18,    .000
CTRIA3, 72,1, 10, 18,  9, 180.000
CTRIA3, 73,1,  9,  2, 10,    .000
CTRIA3, 74,1,178,154,179,    .000
CTRIA3, 75,1,155,179,154,  180.00
CTRIA3, 76,1,154,130,155,    .000
CTRIA3, 77,1,131,155,130,  180.00
CTRIA3, 78,1,130,106,131,    .000
CTRIA3, 79,1,107,131,106,  180.00
CTRIA3, 80,1,106, 82,107,    .000
CTRIA3, 81,1, 83,107, 82,  180.00
CTRIA3, 82,1, 82, 60, 83;    .000
CTRIA3, 83,1, 61, 83, 60,  180.00
CTRIA3, 84,1, 60, 42, 61,    .000
CTRIA3, 85,1, 43, 61, 42,  180.00
CTRIA3, 86,1, 42, 28, 43,    .000
CTRIA3, 87,1, 29, 43, 28,  180.00
CTRIA3, 88,1, 28, 18, 29,    .000
CTRIA3, 89,1, 19, 29, 18,  180.00
CTRIA3, 90,1, 18, 10, 19,    .000
CTRIA3, 91,1,179,155,180,    .000
CTRIA3, 92,1,156,180,155,  180.00
CTRIA3, 93,1,155,131,156,    .000
CTRIA3, 94,1,132,156,131,  180.00
CTRIA3, 95,1,131,107,132,    .000
CTRIA3, 96,1,108,132,107,  180.00
CTRIA3, 97,1,107, 83,108,    .000
CTRIA3, 98,1, 84,108, 83,  180.00
CTRIA3, 99,1, 83, 61, 84,    .000
CTRIA3,100,1, 62, 84, 61,  180.00
CTRIA3,101,1, 61, 43, 62,    .000
CTRIA3,102,1, 44, 62, 43,  180.00
CTRIA3,103,1, 43, 29, 44,    .000
CTRIA3,104,1, 30, 44, 29,  180.00
CTRIA3,105,1, 29, 19, 30,    .000
CTRIA3,106,1,180,156,181,    .000
CTRIA3,107,1,157,181,156,  180.00
CTRIA3,108,1,156,132,157,    .000
CTRIA3,109,1,133,157,132,  180.00
CTRIA3,110,1,132,108,133,    .000
CTRIA3,111,1,109,133,108,  180.00
CTRIA3,112,1,108, 84,109,    .000
CTRIA3,113,1, 85,109, 84,  180.00
```

```
CTRIA3,114,1, 84, 62, 85,    .000
CTRIA3,115,1, 63, 85, 62,  180.00
CTRIA3,116,1, 62, 44, 63,    .000
CTRIA3,117,1, 45, 63, 44,  180.00
CTRIA3,118,1, 44, 30, 45,    .000
CTRIA3,119,1,181,157,182,    .000
CTRIA3,120,1,158,182,157,  180.00
CTRIA3,121,1,157,133,158,    .000
CTRIA3,122,1,134,158,133,  180.00
CTRIA3,123,1,133,109,134,    .000
CTRIA3,124,1,110,134,109,  180.00
CTRIA3,125,1,109, 85,110,    .000
CTRIA3,126,1, 86,110, 85,  180.00
CTRIA3,127,1, 85, 63, 86,    .000
CTRIA3,128,1, 64, 86, 63,  180.00
CTRIA3,129,1, 63, 45, 64,    .000
CTRIA3,130,1,182,158,183,    .000
CTRIA3,131,1,159,183,158, 180.000
CTRIA3,132,1,158,134,159,    .000
CTRIA3,133,1,135,159,134, 180.000
CTRIA3,134,1,134,110,135,    .000
CTRIA3,135,1,111,135,110,  180.00
CTRIA3,136,1,110, 86,111,    .000
CTRIA3,137,1, 87,111, 86, 180.000
CTRIA3,138,1, 86, 64, 87,    .000
CTRIA3,139,1,183,159,184,    .000
CTRIA3,140,1,160,184,159, 180.000
CTRIA3,141,1,159,135,160,    .000
CTRIA3,142,1,136,160,135, 180.000
CTRIA3,143,1,135,111,136,    .000
CTRIA3,144,1,112,136,111, 180.000
CTRIA3,145,1,111, 87,112,    .000
CTRIA3,146,1,184,160,185,    .000
CTRIA3,147,1,161,185,160, 180.000
CTRIA3,148,1,160,136,161,    .000
CTRIA3,149,1,137,161,136, 180.000
CTRIA3,150,1,136,112,137,    .000
CTRIA3,151,1,185,161,186,    .001
CTRIA3,152,1,162,186,161,  180.00
CTRIA3,153,1,161,137,162,    .001
CTRIA3,154,1,186,162,187,    .006
CTRIA3,155,1,177,178,203,  59.999
CTRIA3,156,1,203,178,204,    .000
CTRIA3,157,1,204,205,229,  60.002
CTRIA3,158,1,229,205,230,    .000
CTRIA3,159,1,230,231,251,  60.173
CTRIA3,160,1,251,231,252,    .000
CTRIA3,161,1,252,253,271,  59.999
CTRIA3,162,1,271,253,272,    .000
CTRIA3,163,1,272,273,289,  60.000
CTRIA3,164,1,289,273,290,    .004
CTRIA3,165,1,290,274,273,    .002
CTRIA3,166,1,290,274,291,    .002
CTRIA3,167,1,290,291,305,  59.999
CTRIA3,168,1,274,275,291,  60.000
CTRIA3,169,1,291,293,306,  59.983
CTRIA3,170,1,275,278,292,  59.383
CTRIA3,171,1,257,276,277,  58.875
CTRIA3,172,1,257,258,276,    .000
CTRIA3,173,1,212,213,237,  59.865
CTRIA3,174,1,212,187,213,    .017
CTRIA3,175,1,162,188,187,  59.913
CTRIA3,176,1,162,163,188,    .007
CTRIA3,177,1,137,113,138,    .000
CTRIA3,178,1, 88,114,113, 177.202
CTRIA3,179,1, 88, 90,114,    .009
CTRIA3,180,1, 65, 67, 89,    .013
```

```
CTRIA3,181,1, 46, 48, 66,   1.038
CTRIA3,182,1, 31, 32, 47,    .016
CTRIA3,183,1, 32, 31, 20, 180.000
CTRIA3,184,1, 30, 20, 19,    .000
CTRIA3,185,1, 19, 11, 20,    .000
CTRIA3,186,1, 19, 11, 10,    .000
CTRIA3,187,1, 10,  3, 11,    .000
CTRIA3,188,1,  3, 10,  2, 180.00
CTRIA3,189,1,275,257,256,    .000
CTRIA3,190,1,236,212,211,    .000
CTRIA3,191,1,212,187,186,    .017
CTRIA3,201,2,268,287,267, 149.999
CTRIA3,202,2,284,267,287,  59.999
CTRIA3,203,2,267,284,265, 149.999
CTRIA3,204,2,282,265,284,  59.999
CTRIA3,205,2,265,282,264, 149.999
CTRIA3,206,2,283,264,282,  59.999
CTRIA3,207,2,243,242,264, 180.000
CTRIA3,208,2,264,266,243,  59.999
CTRIA3,209,2,242,245,265, 180.000
CTRIA3,210,2,265,264,242,  60.000
CTRIA3,211,2,245,246,267, 180.000
CTRIA3,212,2,267,265,245,  60.000
CTRIA3,213,2,246,247,268, 180.000
CTRIA3,214,2,268,267,246,  60.000
CTRIA3,215,2,247,248,269, 180.000
CTRIA3,216,2,269,268,247,  59.999
CTRIA3,217,2,219,221,242, 180.000
CTRIA3,218,2,242,243,219,  59.966
CTRIA3,219,2,221,222,245, 180.000
CTRIA3,220,2,245,242,221,  59.966
CTRIA3,221,2,222,223,246, 180.000
CTRIA3,222,2,246,245,222,  59.966
CTRIA3,223,2,223,224,247, 180.000
CTRIA3,224,2,247,246,223,  59.966
CTRIA3,225,2,224,225,248, 180.000
CTRIA3,226,2,248,247,224,  59.966
CTRIA3,227,2,225,226,249, 180.000
CTRIA3,228,2,249,248,225,  60.173
CTRIA3,229,2,192,194,219, 180.000
CTRIA3,230,2,219,220,192,  60.002
CTRIA3,231,2,194,195,221, 180.000
CTRIA3,232,2,221,219,194,  60.000
CTRIA3,233,2,195,196,222, 180.000
CTRIA3,234,2,222,221,195,  60.000
CTRIA3,235,2,196,197,223, 180.000
CTRIA3,236,2,223,222,196,  60.000
CTRIA3,237,2,197,198,224, 180.000
CTRIA3,238,2,224,223,197,  60.000
CTRIA3,239,2,198,199,225, 180.000
CTRIA3,240,2,225,224,198,  60.000
CTRIA3,241,2,199,200,226, 180.000
CTRIA3,242,2,226,225,199,  60.000
CTRIA3,243,2,200,202,227, 180.000
CTRIA3,244,2,227,226,200,  60.002
CTRIA3,245,2, 36, 22, 37,    .000
CTRIA3,246,2, 37, 52, 36, 180.000
CTRIA3,247,2, 52, 37, 54,    .000
CTRIA3,248,2, 54, 73, 52, 180.000
CTRIA3,249,2, 73, 54, 76,    .000
CTRIA3,250,2, 76, 96, 73, 180.000
CTRIA3,251,2, 96, 76,100,    .000
CTRIA3,252,2,100,120, 96, 180.000
CTRIA3,253,2,120,100,125,    .000
CTRIA3,254,2,125,144,120, 180.000
CTRIA3,255,2,201,175,202,    .000
CTRIA3,256,2,176,202,175, 180.000
```

```
CTRIA3,257,2,175,151,176,    .000
CTRIA3,258,2,152,176,151, 180.000
CTRIA3,259,2,151,127,152,    .000
CTRIA3,260,2,128,152,127, 180.000
CTRIA3,261,2,127,103,128,    .000
CTRIA3,262,2,104,128,103, 180.000
CTRIA3,263,2,103, 79,104,    .000
CTRIA3,264,2, 80,104, 79, 180.000
CTRIA3,265,2, 79, 57, 80,    .000
CTRIA3,266,2, 58, 80, 57, 180.000
CTRIA3,267,2, 57, 39, 58,    .000
CTRIA3,268,2, 40, 58, 39, 180.000
CTRIA3,269,2, 39, 25, 40,    .000
CTRIA3,270,2, 26, 40, 25, 180.000
CTRIA3,271,2, 25, 15, 26,    .000
CTRIA3,272,2, 16, 26, 15, 180.000
CTRIA3,273,2, 15,  5, 16,    .000
CTRIA3,274,2,202,176,200,    .000
CTRIA3,275,2,174,200,176,  180.00
CTRIA3,276,2,176,152,174,    .000
CTRIA3,277,2,150,174,152,  180.00
CTRIA3,278,2,152,128,150,    .000
CTRIA3,279,2,126,150,128,  180.00
CTRIA3,280,2,128,104,126,    .000
CTRIA3,281,2,102,126,104,  180.00
CTRIA3,282,2,104, 80,102,    .000
CTRIA3,283,2, 78,102, 80,  180.00
CTRIA3,284,2, 80, 58, 78,    .000
CTRIA3,285,2, 56, 78, 58,  180.00
CTRIA3,286,2, 58, 40, 56,    .000
CTRIA3,287,2, 38, 56, 40,  180.00
CTRIA3,288,2, 40, 26, 38,    .000
CTRIA3,289,2, 24, 38, 26,  180.00
CTRIA3,290,2, 26, 16, 24,    .000
CTRIA3,291,2,200,174,199,    .000
CTRIA3,292,2,173,199,174,  180.00
CTRIA3,293,2,174,150,173,    .000
CTRIA3,294,2,149,173,150,  180.00
CTRIA3,295,2,150,126,149,    .000
CTRIA3,296,2,124,149,126,  180.00
CTRIA3,297,2,126,102,124,    .000
CTRIA3,298,2, 99,124,102,  180.00
CTRIA3,299,2,102, 78, 99,    .000
CTRIA3,300,2, 75, 99, 78,  180.00
CTRIA3,301,2, 78, 56, 75,    .000
CTRIA3,302,2, 53, 75, 56,  180.00
CTRIA3,303,2, 56, 38, 53,    .000
CTRIA3,304,2, 36, 53, 38,  180.00
CTRIA3,305,2, 38, 24, 36,    .000
CTRIA3,306,2,199,173,198,    .000
CTRIA3,307,2,172,198,173,  180.00
CTRIA3,308,2,173,149,172,    .000
CTRIA3,309,2,148,172,149,  180.00
CTRIA3,310,2,149,124,148,    .000
CTRIA3,311,2,123,148,124,  180.00
CTRIA3,312,2,124, 99,123,    .000
CTRIA3,313,2, 98,123, 99,  180.00
CTRIA3,314,2, 99, 75, 98,    .000
CTRIA3,315,2, 74, 98, 75,  180.00
CTRIA3,316,2, 75, 53, 74,    .000
CTRIA3,317,2, 52, 74, 53,  180.00
CTRIA3,318,2, 53, 36, 52,    .000
CTRIA3,319,2,198,172,197,    .000
CTRIA3,320,2,171,197,172,  180.00
CTRIA3,321,2,172,148,171,    .000
CTRIA3,322,2,147,171,148,  180.00
CTRIA3,323,2,148,123,147,    .000
```

```
CTRIA3,324,2,122,147,123,  180.00
CTRIA3,325,2,123, 98,122,    .000
CTRIA3,326,2, 97,122, 98,  180.00
CTRIA3,327,2, 98, 74, 97,    .000
CTRIA3,328,2, 73, 97, 74,  180.00
CTRIA3,329,2, 74, 52, 73,    .000
CTRIA3,330,2,197,171,196,    .000
CTRIA3,331,2,170,196,171, 180.000
CTRIA3,332,2,171,147,170,    .000
CTRIA3,333,2,146,170,147, 180.000
CTRIA3,334,2,147,122,146,    .000
CTRIA3,335,2,121,146,122,  180.00
CTRIA3,336,2,122, 97,121,    .000
CTRIA3,337,2, 96,121, 97, 180.000
CTRIA3,338,2, 97, 73, 96,    .000
CTRIA3,339,2,196,170,195,    .000
CTRIA3,340,2,169,195,170, 180.000
CTRIA3,341,2,170,146,169,    .000
CTRIA3,342,2,145,169,146, 180.000
CTRIA3,343,2,146,121,145,    .000
CTRIA3,344,2,120,145,121, 180.000
CTRIA3,345,2,121, 96,120,    .000
CTRIA3,346,2,195,169,194,    .000
CTRIA3,347,2,168,194,169, 180.000
CTRIA3,348,2,169,145,168,    .000
CTRIA3,349,2,144,168,145, 180.000
CTRIA3,350,2,145,120,144,    .000
CTRIA3,351,2,194,168,192,    .001
CTRIA3,352,2,167,192,168,  180.00
CTRIA3,353,2,168,144,167,    .001
CTRIA3,354,2,192,167,193,    .006
CTRIA3,355,2,228,202,201,    .000
CTRIA3,356,2,228,202,227,    .000
CTRIA3,357,2,250,226,227,    .000
CTRIA3,358,2,250,226,249,    .000
CTRIA3,359,2,270,248,249,    .000
CTRIA3,360,2,270,248,269,    .000
CTRIA3,361,2,288,268,269,    .000
CTRIA3,362,2,288,268,287,    .000
CTRIA3,363,2,304,284,287,    .004
CTRIA3,364,2,304,284,301,    .004
CTRIA3,365,2,301,282,284,    .002
CTRIA3,366,2,301,282,302,    .002
CTRIA3,367,2,313,302,301,    .000
CTRIA3,368,2,302,283,282,    .000
CTRIA3,369,2,311,303,302,   2.824
CTRIA3,370,2,299,286,283,   8.547
CTRIA3,371,2,285,280,266,  14.396
CTRIA3,372,2,266,262,280,    .000
CTRIA3,373,2,220,217,240,  59.865
CTRIA3,374,2,220,193,217,    .017
CTRIA3,375,2,167,190,193,  59.913
CTRIA3,376,2,167,165,190,    .007
CTRIA3,377,2,144,125,142,    .000
CTRIA3,378,2,100,118,125, 177.202
CTRIA3,379,2,100,101,118,    .009
CTRIA3,380,2, 76, 77, 94,    .013
CTRIA3,381,2, 54, 55, 71,   1.038
CTRIA3,382,2, 37, 34, 50,    .016
CTRIA3,383,2, 37, 34, 22,    .016
CTRIA3,384,2, 36, 22, 24,    .000
CTRIA3,385,2, 24, 13, 22,    .000
CTRIA3,386,2, 24, 13, 16,    .000
CTRIA3,387,2, 16,  7, 13,    .000
CTRIA3,388,2, 16,  7,  5,    .000
CTRIA3,389,2,283,266,264,    .000
CTRIA3,390,2,243,220,219,    .000
```

```
CTRIA3,391,2,220,193,192,     .017
CQUAD4  192     1       305     291     306     307     0.
CQUAD4  193     1       291     275     292     293     0.
CQUAD4  194     1       275     257     277     278     0.
CQUAD4  195     1       236     238     258     257     0.
CQUAD4  196     1       236     212     237     238     0.
CQUAD4  197     1       137     138     163     162     0.
CQUAD4  198     1       65      89      90      88      0.
CQUAD4  199     1       46      66      67      65      0.
CQUAD4  200     1       31      47      48      46      0.
CQUAD4  392     2       313     302     311     314     0.
CQUAD4  393     2       302     283     299     303     0.
CQUAD4  394     2       283     266     285     286     0.
CQUAD4  395     2       243     244     262     266     0.
CQUAD4  396     2       243     220     240     244     0.
CQUAD4  397     2       144     142     165     167     0.
CQUAD4  398     2       76      94      101     100     0.
CQUAD4  399     2       54      71      77      76      0.
CQUAD4  400     2       37      50      55      54      0.
PSOLID  3       3
CHEXA   401     3       2       3       4       1       5       7       +H401
+H401   8       6
CHEXA   402     3       3       11      12      4       7       13      +H402
+H402   14      8
CHEXA   403     3       11      20      21      12      13      22      +H403
+H403   23      14
CHEXA   404     3       20      32      33      21      22      34      +H404
+H404   35      23
CHEXA   405     3       32      47      49      33      34      50      +H405
+H405   51      35
CHEXA   406     3       47      48      68      49      50      55      +H406
+H406   69      51
CHEXA   407     3       48      66      70      68      55      71      +H407
+H407   72      69
CHEXA   408     3       66      67      91      70      71      77      +H408
+H408   92      72
CHEXA   409     3       67      89      93      91      77      94      +H409
+H409   95      92
CHEXA   410     3       89      90      115     93      94      101     +H410
+H410   116     95
CHEXA   411     3       90      114     117     115     101     118     +H411
+H411   119     116
CHEXA   412     3       114     113     139     117     118     125     +H412
+H412   140     119
CHEXA   413     3       113     138     141     139     125     142     +H413
+H413   143     140
CHEXA   414     3       138     163     164     141     142     165     +H414
+H414   166     143
CHEXA   415     3       163     188     189     164     165     190     +H415
+H415   191     166
CHEXA   416     3       188     187     214     189     190     193     +H416
+H416   215     191
CHEXA   417     3       187     213     216     214     193     217     +H417
+H417   218     215
CHEXA   418     3       213     237     239     216     217     240     +H418
+H418   241     218
CHEXA   419     3       237     238     259     239     240     244     +H419
+H419   260     241
CHEXA   420     3       238     258     261     259     244     262     +H420
+H420   263     260
CHEXA   421     3       258     276     279     261     262     280     +H421
+H421   281     263
CHEXA   422     3       276     277     294     279     280     285     +H422
+H422   295     281
CHEXA   423     3       277     278     296     294     285     286     +H423
+H423   297     295
CHEXA   424     3       278     292     298     296     286     299     +H424
```

```
+H424   300     297
CHEXA   425     3       292     293     308     298     299     303     +H425
+H425   309     300
CHEXA   426     3       293     306     310     308     303     311     +H426
+H426   312     309
CHEXA   427     3       306     307     315     310     311     314     +H427
+H427   316     312
FORCE   1       2       0       7.4113520.      -1.000000.
FORCE   1       5       0       7.4113520.      -1.000000.
FORCE   1       9       0       14.822700.      -1.000000.
FORCE   1       15      0       14.822700.      -1.000000.
FORCE   1       17      0       14.822700.      -1.000000.
FORCE   1       25      0       14.822700.      -1.000000.
FORCE   1       27      0       14.822700.      -1.000000.
FORCE   1       39      0       14.822700.      -1.000000.
FORCE   1       41      0       14.822700.      -1.000000.
FORCE   1       57      0       14.822700.      -1.000000.
FORCE   1       59      0       14.822700.      -1.000000.
FORCE   1       79      0       14.822700.      -1.000000.
FORCE   1       81      0       14.822700.      -1.000000.
FORCE   1       103     0       14.822700.      -1.000000.
FORCE   1       105     0       14.822700.      -1.000000.
FORCE   1       127     0       14.822700.      -1.000000.
FORCE   1       129     0       14.822700.      -1.000000.
FORCE   1       151     0       14.822700.      -1.000000.
FORCE   1       153     0       14.822700.      -1.000000.
FORCE   1       175     0       14.822700.      -1.000000.
FORCE   1       177     0       10.48115-.707101-.7071130.
FORCE   1       201     0       10.48115-.707101-.7071130.
FORCE   1       203     0       14.82246-1.000000.      0.
FORCE   1       204     0       14.82331-1.000000.      0.
FORCE   1       227     0       14.82331-1.000000.      0.
FORCE   1       228     0       14.82246-1.000000.      0.
FORCE   1       229     0       14.82245-1.000000.      0.
FORCE   1       230     0       14.87379-1.000000.      0.
FORCE   1       249     0       14.87379-1.000000.      0.
FORCE   1       250     0       14.82245-1.000000.      0.
FORCE   1       251     0       14.82417-1.000000.      0.
FORCE   1       252     0       14.77196-1.000000.      0.
FORCE   1       269     0       14.77196-1.000000.      0.
FORCE   1       270     0       14.82417-1.000000.      0.
FORCE   1       271     0       14.82245-1.000000.      0.
FORCE   1       272     0       14.82246-1.000000.      0.
FORCE   1       287     0       14.82246-1.000000.      0.
FORCE   1       288     0       14.82245-1.000000.      0.
FORCE   1       289     0       14.82331-1.000000.      0.
FORCE   1       290     0       14.82331-1.000000.      0.
FORCE   1       301     0       14.82331-1.000000.      0.
FORCE   1       304     0       14.82331-1.000000.      0.
FORCE   1       305     0       11.46515-1.000000.      0.
FORCE   1       307     0       4.053924-1.000000.      0.
FORCE   1       313     0       11.46515-1.000000.      0.
FORCE   1       314     0       4.053924-1.000000.      0.
ENDDATA
```

APPENDIX B

Calculation of Initial Tension in Composite Layup

Initial stress in carbon fibers $= 50{,}000$ psi

Area of cross-section of 6K tow $= 3.77 \times 10^{-4}$ in^2

Force in cable (tension) $= \sigma$ A

$$T = 50{,}000 \times 3.77 \times 10^{-4}$$

$$T = 18.85 \text{ lb}$$

For side AB (see Fig. B.1(c)), the horizontal terms cancel each other.

Total tension $= 2 \times T \sin 60^o$

$$= 2 \times 18.85 \times 0.866 = 32.649 \text{ lb}$$

Line load along AB = (total tension × no. of fibers)/radius of arm (=100)

$$= (32.649 \times 100)/(1000/25.4) = 82.93 \text{ lb/in}$$

$$= 82.93 \times (1/2.2046) \times (1/25.4) \text{ kg/mm}$$

$$= 1.481 \text{ kg/mm}$$

For side AC (see Fig. B.1(c))

$T + 2T \cos 60^o = 2T = 2 \times 18.85 = 37.7$ lbs

Line load $= (37.7 \times 100)/(1000/25.4) = 95.758$ lb/in

$$= 1.71 \text{ kg/mm}$$

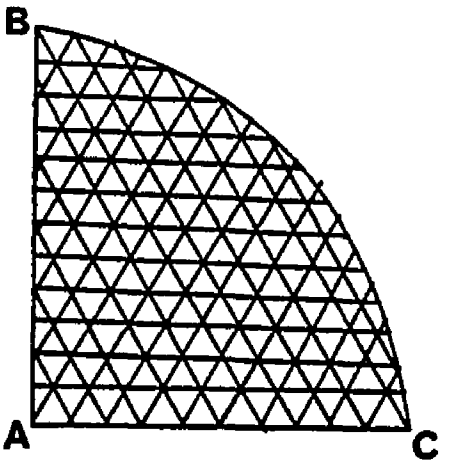

Figure B.1(a)

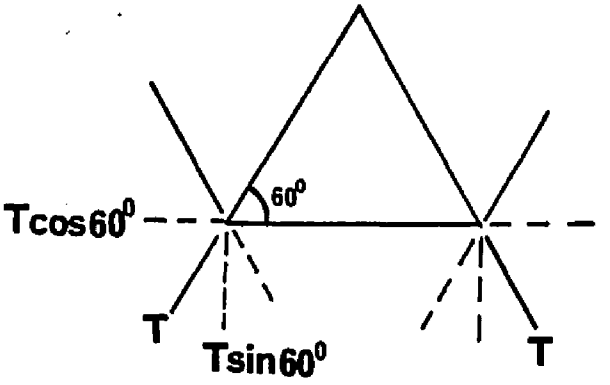

Figure B.1(b)

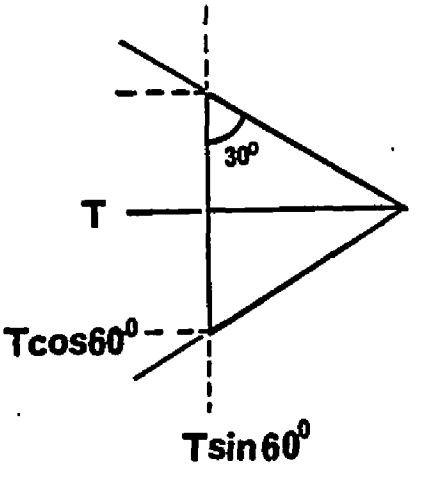

Figure B.1(c)

Figure B.1 Fiber Orientation for Initial Tension Computation:
(a) Fiber Arrangement in the Quarter Model,
(b) One element on Side A-C and,
(c) One element on Side A-B .

APPENDIX C

EXPERIMENTAL CONSTRUCTION

The experimental construction proceeded simultaneously with the analytical calculations. The concept of flat reflectors was extended to curved reflectors. Four parabolic reflectors were built to prove the concept of advanced-composite membrane supports. All of these have a ring frame, 1.1 m in diameter. The tubular ring frame is anodized mild steel. A positive mold (made of Plaster of Paris) was used. The ratio of focal length to diameter, the F number, was 0.4, and represented a realistic situation. Both radial and cirumferential fiber reinforcements were used. Graphite fibers with epoxy resin were used for the composite fibers. Two different resins were used. The choice was determined by a careful balance of pot life (working ability for several hours before it starts to harden), flexibility during use (varying viscosity), strength and hardness after cure, and the cure time (varying from a few hours to almost a week, depending on the resin/hardner ratio). Surprisingly, not much data is available on these aspects which vary from application to application. For example, the non-continuous fiber mesh influenced the resin handling and cure processes.

The curved reflectors employed the ECP 244 reflector film. For a diameter of 1.2 m, the loads required to stretch the membrane can be thousands of pounds, and the process requires a carefully controlled uniform load distribution to avoid differential stressing. A simple alternative to applying tension with sophisticated equipment was used: The reflector film was built up in sections much like umbrella sections. Twelve triangular sectors were selected for the film layup. 3-M supplied adhesive tape (0.5 inch wide) that was very thin and matched the reflectivity of the

main film. The finished product showed remarkable improvement over the earlier flat reflectors, which were built with a continuous piece of film. The graphite-fiber fishnet "basket structure" was made on the mold. After the resin hardened, the film was bonded to the "basket structure" in a stressed mode. The membrane at the back was bonded last.

The 1.1-m diameter module weighed approximately six pounds (2.6 kg/m^2), proving the concept of light weight, which is one of the objectives of this research.

Figure C.1 Photograph of Parabolic Dish Showing Radial and Circumferential Fiber Reinforcement

Figure C.2 Photograph of Plaster of Paris Mold and
a Finished Parabolic Dish Reflector

APPENDIX D

Error in Initial Tension Computation

The calculation of initial tension in the composite membrane layup is given in Appendix B. Due to the assumptions made earlier in computing the tension, asymmetrical tension values were obtained. The initial tension was recomputed and is shown below:

For side AB,

Number of fibers in the 0^o direction = $N_{(0)}$ = side AB/d

where d is the fiber spacing.

Therefore, $N_{(0)} = 1000/10 = 100$

Number of fibers in the 60^o direction = $N_{(60)}$ = side AB/(d/sin 60^o)

$$N_{(60)} = 1000/(10/\sin 60^o) = 86.6$$

Similarly,

Number fibers in the -60^o direction = $N_{(-60)}$ = side AB/(d/sin30^o)

$$N_{(-60)} = 1000/(10/\sin 30) = 50.0$$

Force in each fiber as shown in Appendix B = 18.85 lb

Force in side AB, due to 0^o fibers = $100 \times 18.85 = 1885.00$ lb

Force in side AB, due to 60^o fibers = $86.6 \times 18.85 = 1632.41$ lb

Force in side AB, due to -60^o fibers = $50 \times 18.85 = 942.5$ lb

Resolving and summing the horizontal and vertical components,

Horizontal component = 3172.46 lb and,

Vertical component = 597.48 lb.

Similarly, for side AC

There are no fibers in the 0^o direction.

Number of fibers in the 60^o direction = 50, and

Number of fibers in the -60^o direction = 86.6.

Total force on side AC, due to 60^o fibers = 942.5 lb, and

due to -60^o fibers = 1632.41 lb.

Resolving and summing the forces,

Horizontal component = 345 lb, and

Vertical component = 2230 lb.

The resultant forces are shown in Fig. D.1.

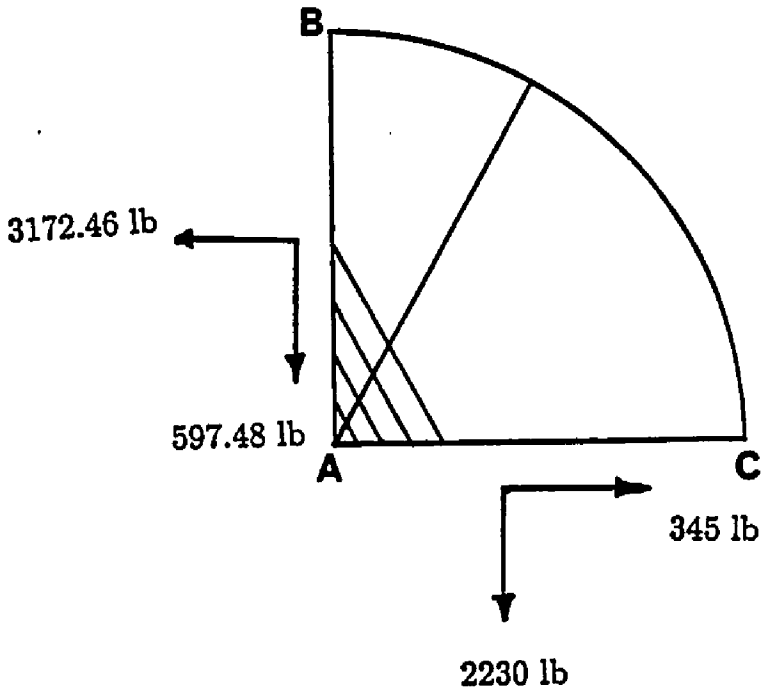

Figure D.1 Quarter Model with Recomputed Initial Tension

REFERENCES

1. Murphy, L. M., Technical and Costs Benefits of Lightweight Stretched-Membrane Heliostats, SERI/TR-253-1818, Solar Energy Research Institute, Golden, Colo., 1983

2. Truscello, V. C., Status of Parabolic Dish Concentrators, Jet Propulsion Laboratory, Pasadena, Calif., 1980.

3. Butler, B. L., Light Weight Diaphragm Mirror Module System for Solar Collectors, U.S. Patent 4,511,215.

4. Murphy, L. M., and Sallis, D. V., Analytical Modeling and Structural Response of a Stretched-Membrane Reflective Module, SERI/TR-253-2101, DE84013004, Solar Energy Research Institute, Golden, Colo., June 1984.

5. Murphy, L. M., A Variational Approach for Predicting the Load Deformation Response of a Double Stretched Membrane Reflector Module, SERI/TR-253-2626, DE85016873, Solar Energy Research Institute, Golden, Colo., October 1985.

6. Murphy, L. M., Anderson, J. V., Short, W., and Wendelin, T., System Performance and Cost Sensitivity Comparisons of Stretched-Membrane Heliostat Reflectors with Current Generation Glass/Metal Concepts, SERI/TR-253-2694, DE85016892, Solar Energy Research Institute, Golden, Colo., December 1985.

7. Wood, L. R., Single, Stretched-Membrane, Structural Module Experiments, SERI/TR-253-2736, DE86004433, Solar Energy Research Institute, Golden, Colo., February, 1986.

8. Joshi, S. P., and Murphy, L. M., Large Axisymmetric Deformation of a Laminated Composite Membrane, Private Communication.

9. Soedel, W., Vibration of Plates and Shells, Marcel Dekker Inc., New York, 1981.

10. Nielan, P. E., Large Elastic Deformation of Nonlinear Axisymmetric Membranes: A Variational Approach, Report No. DE83-001851, Sandia Laboratories, Livermore, Calif., November 1982.

11. Cook, W. A., A Finite Element Model for Nonlinear Shells of Revolution, International Journal for Numerical Methods in Engineering, Vol. 18, January 1982, pp. 135-149.

12. Fried, I., Finite Element Computation of Large Rubber Membrane Deformations, International Journal for Numerical Methods in Engineering, Vol. 18, May 1982, pp. 653-660.

13. Ramohalli K. N. R., Butler, B. L., and Visvanathan G., Advanced Composites for Stressed-Membrane Heliostats, Energy, Vol. 12, No. 3/4, pp. 245-259, 1987.

14. MSC/NASTRAN Manuals, Version 63, The McNeal-Schwendler Corp., Los Angeles, Calif.

15. GIFTS Users Reference Manual, Research and Development, Casa Gifts, Inc., Tucson, Ariz., 1985.

15. Jones, R. M., Mechanics of Composite Materials, McGraw-Hill Book Company, New York, 1975.

16. Handbook of Industrial Materials, Trade and Technical Press Ltd., England.

17. Ashton, J. E., Halpin, J. C., Petit, P. H., Primer on Composite Materials Analysis, Technomic Publications, Technomic Publishing Co. Inc., Conn.

18 Hand Book of Composites, Von Nostrand Co., New York, Edited by: George Lubin.